# Extreme rainfall events over the Pongola-Mtamvuna Water Management Area of South Africa


**By**

**Nomvula Bongekile Mpungose**



**Thesis submitted in fulfilment of the requirements for the Master's degree in**

**Ocean and Atmosphere Science**


**In the Department of Oceanography**

**University of Cape Town**


**June 2021**

# Plagiarism declaration

I understand that plagiarism is a serious form of academic dishonesty and fully declare that each significant contribution to, and quotation in, this thesis from the work of other people has been properly acknowledged. The content of this thesis represents my own work, I have not allowed, and will not allow, anyone to copy my work with the intention of passing it off as his or her own work.

Signature: Signed by candidate Date: 17/06/2021

# Acknowledgements

I would like to extend my gratitude to my amazing supervisors Professor Chris Reason and Dr Ross Blamey for their much appreciated input, guidance, and support from the beginning of this journey up to this point. Thank you! This journey would have been impossible without funding, I am grateful to the National Research Foundation (ACCESS) and the Postgraduate Funding Office for providing financial support towards this thesis. Thanks to the South African Weather Service for granting me the use of their station data used in Chapter 4. I would also like to thank my wonderful colleagues (Wanjiru, Precious, Dedricks, Wade and Ramontsheng) for always assisting me whenever I needed it. Finally to all my loved ones, thank you to each and every one of you for always uplifting me throughout this journey!

# Abstract

Subtropical southern Africa experiences substantial rainfall variability both spatially and temporally, due to regional orography, geographic position, and local sea-surface temperatures. Extreme weather conditions such as droughts and floods are not uncommon and can result in both positive and negative socio-economic impacts. The Pongola-Mtamvuna Water Management Area (PM) located over north-eastern South Africa consists of communities that depend on rain-fed agriculture, as well as an inter-linked ecosystem and fresh water bodies that are dependent on rainfall. Extreme rainfall events and the systems that produce them are still not well understood, therefore, a detailed analysis of such events can contribute to an improved understanding and management of their associated risks.

Here, the main focus is on the summer rainy season (October – March), rainfall variability is examined using CHIRPS daily rainfall data covering a period of thirty-seven years from 1981 – 2018. Extreme rainfall events are identified and classified for the PM area. The analysis points to the highest rainfall amounts typically occurring over low-lying coastal areas and near mountainous regions. About 60% of the extreme rainfall events were associated with tropical lows (40%) and MCS (20%). Cut-off lows (18%), cloud bands (16%), and tropical cyclones (6%) contributed to the remaining proportion. The highest frequency of events occurred during late summer months (January – March) when tropical lows and occasionally, tropical cyclones are more common. Rainfall over the PM has a statistically significant relationship with ENSO, most of the seasons with below-average rainfall and extreme events coincided with El Niño conditions. Odd cases where this was the opposite were more influenced by regional circulation anomalies which acted to enhance or reduce moisture over the land-mass thereby increasing conditions favourable/unfavourable for rainfall over the region.

# Table of contents

# List of Figures and Tables

# Introduction

The Pongola-Mtamvuna Water Management Area (PM) (**Figure 1**) is located over eastern South Africa, covers northern KwaZulu-Natal (KZN), most of Swaziland and part of Mpumalanga. The PM region is of local economic importance due to contributions towards the agricultural and tourism industries. The region receives most of its rainfall during the austral summer from October – March, with rainfall peaks typically occurring in December to January. Most of the rainfall over this region is of convective origin (Blamey and Reason, 2009) with considerable spatial and temporal variability owing to the presence of the warm Agulhas current and favourable atmospheric circulation patterns (Blamey and Reason, 2013). A renowned Ramsar and World Heritage site, the iSimangaliso Wetland Park, and the largest freshwater lake in South Africa, Lake Sibayi are confined within the Maputaland Coastal Plain (Weitz and Demlie, 2014). The region boasts two major interlinked ecosystems (St. Lucia and Kosi Bay) and freshwater water bodies (Briggs, 2008) that mostly depend on groundwater (Kelbe and Germishuyse, 2010). Not only is the PM rich in tourism and development, but its ecosystem consists of a limited extent of habitats rich in mangrove forests, coral reefs, and raffia-palm forests, this is discussed further in Fairer-Wessels (2017).

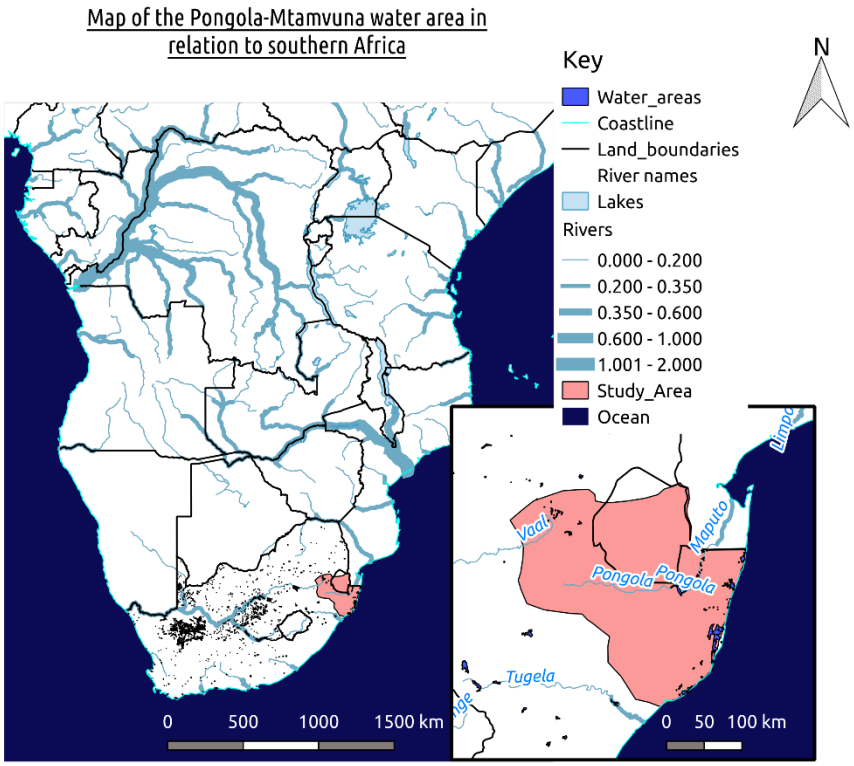


**Figure 1:** Map of southern Africa showing the Pongola-Mtamvuna Water Management Area (pink shaded polygon) over parts of northern KwaZulu-Natal, Swaziland and south-eastern Mpumalanga. The sources for the river flow, based on SANBI metadata, are indicated in blue lines and shading. Produced with QGIS.

In recent years, the PM region has been severely affected by droughts which have devastating socio-economic impacts, especially in regions where water input is completely reliant on precipitation. For example, the decrease in the lake area of Lake Sibaya situated in northern KZN is argued to be related to long-term climate change (Nsubuga *et al*., 2019). Although changes in the lake also depend on factors such as water management practices as well as farming activities in the lake basin, they argued that it was difficult for lake levels to recover after years of below-average rainfall, even after extreme rainfall events. Serious droughts have also been reported to increase the salinity of Lake St Lucia, killing off the shoreline vegetation (Fairer-Wessels, 2017). By contrast, extreme rains due to the activity of severe weather systems often result in flooding

over the region. A good example of this occurred in January 1984, when tropical cyclone Domoina caused heavy rains over northern KZN and parts of Mozambique and Swaziland with a loss of human life and thousands of livestock as well as damage to crops and infrastructure (Steinke and Ward, 1989, Jury *et al*., 1993). A more recent flood event occurred in April 2019 over coastal KZN where 71 deaths were reported and an estimated number of 1400 people were displaced (Bopape *et al*., 2021); approximately USD71 million worth of facilities and infrastructure were destroyed. However, these extreme rainfall events also positively impact lakes by increasing their water levels, especially in this region because the interconnected hydrologic system causes automatic transmission into surface water bodies and wetlands, including the conservation areas (Ramjeawon *et al*., 2020).

Southern Africa is prone to high impact events such as droughts, severe storms and floods (Reason *et al*., 2005, New *et al*., 2006, Reason, 2017, Rapolaki *et al*., 2019). Heavy rainfall events may be associated with convective weather systems which can range from single-cell thunderstorms through to more complex, larger scale systems such as tropical lows, cut-off lows and mesoscale convective systems (MCS). Tropical-extratropical cloud bands or tropical temperature troughs (TTT) have also been associated with heavy rainfall over southern Africa during summer (Fauchereau *et al*., 2009, Hart *et al*., 2010, Manhique *et al*., 2011). While tropical lows are important contributors to rainfall over many parts of southern Africa north of about 25$^{o}$S (Malherbe *et al*., 2012, Howard *et al*., 2019, Rapolaki *et al*., 2019), tropical cyclones tend to be important mainly in the Madagascan and Mozambique region. Occasionally, tropical cyclones land-falling on Mozambique can penetrate anomalously far inland with substantial rainfall a long way from the Mozambique Channel such as Eline in 2000 (Reason and Keibel, 2004). Studies focusing on MCSs or mesoscale convective complexes (MCCs) (Blamey and Reason, 2009, Blamey and Reason, 2013) have also shown that these systems contribute significantly to the summer rainfall over south-eastern Africa. Cut-off lows, being mid-latitude in origin, tend to be more important over the southern South Africa although they can also contribute to some heavy rainfall events further north such as the Limpopo River Basin (Rapolaki *et al*., 2019). These systems are most common during the transition seasons over southern Africa (Favre *et al*., 2013, Favre *et al*., 2012).

In addition to understanding the rainfall patterns of individual extreme events, their contribution to seasonal totals also needs to be studied. Regional and global trends in daily precipitation extremes suggest that there may be differences in the variability of daily and annual rainfall amounts, such that increasing daily rainfall amounts over some regions are not always followed by an increase in the annual mean rainfall (New *et al*., 2006, Kruger and Nxumalo, 2017, Du *et al*., 2019). Over southern and West Africa, average daily rainfall and intensity have increased however, the total rainfall and frequency of heavy rain days are decreasing (New *et al*., 2006). According to Kruger and Nxumalo (2017) increases in annual rainfall over the south and central parts of South Africa were partially due to increases in individual extreme precipitation events.

Over the PM, little to no research has been done on the variability of extreme rainfall events. As a region that consists of important freshwater systems and poor rural communities reliant on rain-fed agriculture, information on the variability of extreme events over the PM is crucial to forecasters, farmers, and disaster management officers to help improve mitigation measures and provide better projections of such events in future climate. Furthermore, land-use planning and decisions outside of conservation areas require accurate information to help reduce negative impacts on water resources. Therefore, the focus of this study is on extreme rainfall events over the PM and associated weather systems. Focus is also placed on understanding how some of the common large-scale modes of climate variability, such as ENSO and SAM, influence the frequency of extreme rainfall events in the region.

# Chapter 1 Literature review

## *1.1 The climate of southern Africa*

Southern Africa, south of 15°S, is a semi-arid region mainly experiencing its larger rainfall amounts in the austral summer half of the year (Richard *et al*., 2001, Crétat *et al*., 2012, Reason, 2017). The January–March season contributes more than 40% to the total annual rainfall over the region, except in southwestern South Africa (Richard *et al*., 2001). Regions relying on rain-fed agriculture are sensitive to rainfall variability such that large deviations from the mean seasonal cycle (floods or droughts) may have severe socio-economic impacts (Crétat *et al*., 2012). Parts of South Africa are characterized by complicated patterns of seasonality which reflects the year-to-year fluctuations in the seasonal cycle and the differences in the atmospheric dynamics that produce rainfall (Nicholson, 2000). It is therefore important to understand factors producing the mean climate of a region as well as the large-scale aspects of the general atmospheric circulation that control temporal variability of rainfall.

### *1.2. Regional atmospheric circulation*

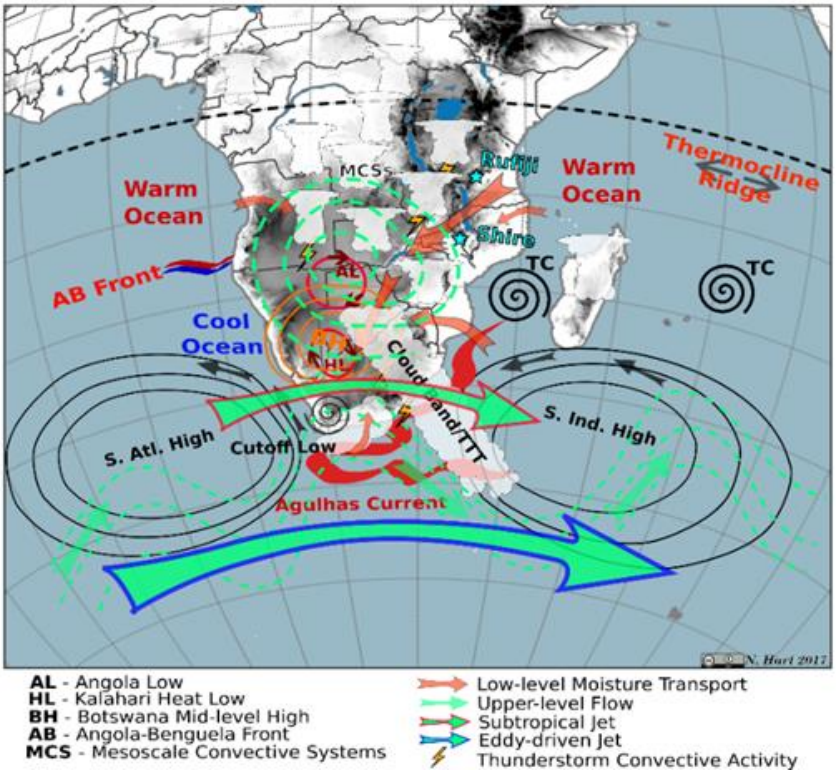


**Figure 2:** A schematic detailing the key circulation processes over southern Africa. AL (Angola Low) HL (Kalahari Heat Low), BH (Botswana mid-level High), AB (Angola-Benguela Front), and MCS (Mesoscale Convective Systems). © Dr Neil C.G. Hart.

**Figure 2** shows the key circulation processes over southern Africa. The Intertropical Convergence Zone (ITCZ) is an important component of general circulation. Nicholson (2018) suggested that the term tropical rain-belt should be used in place of the ITCZ for tropical landmasses, and particularly over Africa except for coastal areas where trade winds are influential. The term tropical rain-belt is used in this study. This band of low pressure shifts southwards in January and northwards during July/August (18° to 20°N), separating the northeast trades from the so-called southwest monsoon flow (Nicholson, 2000). A zone of prevailing high pressure is observed over southern Africa during this time. In January, the southwards penetration of the tropical rain-belt into the Southern Hemisphere is accompanied by a low pressure system over southern Africa. In February, this system reaches its southernmost position over land when it lies across Madagascar

(Barimalala *et al*., 2020) and some south-eastern African regions (Reason *et al*., 2006). The movement of the tropical rain-belt is also linked to warming and cooling of the Atlantic Ocean and south-westward shift of the Botswana High (Reason *et al*., 2006, Reason, 2016). The latter is thermally induced in response to heat released by tropical regions of high precipitation; this circulation feature is prominent at mid-tropospheric levels over southern Africa and typically becomes evident in August (Reason, 2016). In spring, it strengthens and shifts southwards, reaching its maximum intensity in February (Reason, 2016, Driver and Reason, 2017). A stronger Botswana High is associated with reduced summer rainfall over subtropical southern Africa and it has been suggested that the current state of this feature may provide useful information to monitor and evaluate summer rainfall and circulation anomalies over the subcontinent (Blamey *et al*., 2018).

Southern African climate is also modulated by two distinct high-pressure cells; the South Atlantic Subtropical High Pressure and the South Indian Ocean High Pressure (Roy and Rouault, 2013). The former can ridge in behind cold fronts, causing them to move further inland while the latter forms one of the two dominant low-level circulation features (Blamey *et al*., 2018) that drive moisture convergence to support convective precipitation in the region. According to Blamey *et al*. (2018), the zonal wind convergence between the tropical Atlantic westerlies, southwest Indian Ocean easterlies, and north-easterlies from the equatorial western Indian Ocean form the boundary of the South Indian Ocean Convergence Zone (SIOCZ). This convergence zone is associated with enhanced summer rainfall over the eastern subcontinent modulated by the Mozambique Channel Trough (MCT) within this region (Barimalala *et al*., 2018, 2020). The MCT, defined as the area-average of the relative vorticity at 850 hPa in the southern Mozambique Channel (35–44°E, 16–26°S) (Barimalala *et al*., 2018) moderates moisture transport from the Southwest Indian Ocean to the southern African landmass and first becomes evident in December. It strengthens until it reaches its maximum intensity in February (Barimalala *et al*., 2018), after which it gradually becomes weak and less apparent by the start of May. Munday and Washington (2017) found that a weak MCT coincided with a stronger Angola Low and excessive rainfall over southern Africa through enhanced direct moisture inflow to the subcontinent.

The Angola Low acts as the source region for the tropical-extratropical cloud bands (Todd and Washington, 1999). This low pressure system forms in response to high surface temperatures in the Angola region and can be identified in the mean climate from the start of spring (October) between 16–20°S and 18–22°E (Todd and Washington, 1999, Munday and Washington, 2017). According to Munday and Washington (2017), the Angola Low and the subcontinental heat low are barely distinguishable during October – November; however, as the season progresses into the core summer (December–February) the heat low becomes distinct from the Angola Low as it shifts south into the Kalahari (now the Kalahari heat low). At this stage in the season, the Angola Low is identifiable as a tropical low rather than a heat low, as it is not capped by midlevel subsidence (Munday and Washington, 2017). Evidence indicates that modulations of the Angola Low, related to tropical southeast Atlantic SSTs, may significantly influence summer rainfall over larger parts of southern Africa, particularly Angola, Namibia, and sometimes also South Africa (Rouault *et al*., 2003, Cook *et al*., 2004). Thus, increased (decreased) near-surface westerlies off the tropical southeast Atlantic to its northwest stronger result in a stronger (weaker) Angola Low, leading to more (less) low-level moisture in the source region for the cloud bands (Rouault *et al*., 2003).

### *1.3. Modes of climate variability*

El Niño Southern Oscillation (ENSO) is the main driver of interannual variability of rainfall over southern Africa (Lindesay, 1988, Reason *et al*., 2000, Fauchereau *et al*., 2009, Roy and Rouault, 2013, Blamey *et al*., 2018). Nicholson and Kim (1997) found the strongest ENSO signals over eastern equatorial and south-eastern Africa; however, much larger sectors of Africa were also affected. They further indicated that the rainfall response was more intense, consistent, and more spatially and temporally coherent during El Niño events. El Niño phase is commonly associated with drought (Nicholson and Kim, 1997, Blamey *et al*., 2018) but there are nonlinear relationships between El Niño and southern African climate (Fauchereau *et al*., 2009). The contrasting El Niño events of 1997/8, 2009/10, and 2015/16 are some of the examples that demonstrates this nonlinearity (Reason and Jagadheesha, 2005, Blamey *et al*., 2018, Driver *et al*., 2019). Reason and Jagadheesha (2005) highlighted that the lack of a severe drought over southern Africa during the very strong 1997/8 El Niño event, was mostly due to the unexpectedly strong Angola Low that occurred during this summer. Typically, the Angola Low strengthens (weakens) during La Niña

(El Niño) events (Reason and Jagadheesha, 2005). It has also been previously suggested that ENSO modulates the rainy season such that the strongest response to ENSO occurs either before or after the core of the rainy season (Nicholson and Kim, 1997). ENSO response is most intense in south-eastern Africa, where maximum response occurs during the rainiest months (Nicholson and Kim, 1997). Favre *et al*. (2013) also found that the development and maturity stage of La Niña (El Niño) events occurred during austral spring and summer. Modes of SST variability modulate response to ENSO (Hoell *et al*., 2017), for example, the northwest-southeast diagonally oriented cold SST anomaly observed from the southern Mozambique Channel to the southwest Indian Ocean during two La Niña summers (1989, 2012) caused unfavourable rainfall conditions over the mainland (Barimalala *et al*., 2018).

The subtropical Indian Ocean Dipole (SIOD) has been previously identified as an important source of ocean–atmosphere variability in the southern Indian Ocean (Behera and Yamagata, 2001). There is evidence that ENSO and SIOD phase combinations have an influence on the southern Africa precipitation response (Hoell *et al*., 2017); however Behera and Yamagata (2001) have also suggested that SIOD phases exhibit variations independent of the synchronous ENSO phase. A positive correlation between the SIOD and rainfall is typical over a wide region of the southern African landmass (Behera and Yamagata, 2001, Reason, 2001). A stronger precipitation response is observed when SIOD and Nino 3.4 indices have opposite signs, which also relates to observed SST anomaly expressions (Hoell *et al*., 2017). However, in the case of the 2009/2010 El Niño, wetter conditions were experienced over southern Africa despite the observed regional SST anomalies which were unfavourable for rainfall (Driver *et al*., 2019). The occurrence of a negative SIOD at the same time as an El Niño event is expected to enhance drought conditions over the landmass (Hoell *et al*., 2015, 2017).

The Southern Annular Mode (SAM) is the leading mode of atmospheric low-frequency variability south of 20°S (Reason and Rouault, 2005, Pohl and Fauchereau, 2012); it is a zonally symmetric structure with synchronous anomalies of opposite signs in Antarctica and the mid-latitudes (Marshall, 2003). Regional impacts of SAM on rainfall show that the positive SAM phase is associated with increased precipitation over most of southern Africa (Gillett *et al*., 2006),

especially over western South Africa. (Reason and Rouault, 2005). A correlation between SAM and ENSO detailed in Pohl *et al*. (2010) indicates that El Niño (La Niña) events tend to coincide with the negative (positive) phase of SAM. When the influence of both phenomena is isolated, the positive SAM phase is associated with more abundant daily rainfall over central South Africa at the intra-seasonal time scale (Pohl *et al*., 2010). However, this relationship is weakened during El Niño years but particularly strong during La Niña events and, to a smaller extent, neutral years. Pohl *et al*. (2010) also investigated the role of SAM at the interannual time scale and found that the contribution of SAM to modulating the rains is barely significant if the ENSO influence is eliminated. Considering the linear dependency between these two modes of climate variability is important to avoid biased diagnostics (Pohl *et al*., 2010).

### *1.4. The role of the surrounding oceans on southern African rainfall*

Rainfall regime is also very dependent on seasonal changes in the air circulations controlling the local atmosphere and sea surface temperature changes from the adjacent oceans (Washington and Preston, 2006). According to (Reason, 2017), rainfall is highest near the east coast, where the adjacent SSTs are warmest. For example, the poleward flowing warm Agulhas Current near the east coast of southern Africa causes high latent heat fluxes, thereby transferring more moisture to the atmosphere than the surrounding waters (Rouault *et al*., 2003), this leads to local storm intensification (Singleton and Reason, 2006, 2007).

An investigation of the impacts of SST variability on the MCT indicated that a dipole-like SST anomaly pattern in the Indian Ocean (8°–40°S) was evident and coincided with strong MCT years. A widespread decline in JFM rainfall was observed over most of southern Africa while the Mozambique Channel, parts of Madagascar, and coastal Mozambique indicated a significant increase in rainfall (Barimalala *et al*., 2020). Although the impacts of the MCT in the frequency and distribution of rainfall events is not well understood (Cook *et al*., 2004), the previous work of Munday and Washington (2017) suggests that the positive SST anomalies in the Mozambique Channel and near the subcontinent weaken the trough (Barimalala *et al*., 2020) which in turn, strengthens the Angola Low and favours the increase in rainfall over the subcontinent.

On the other hand, marked annual cycle in winds and SST over the southeast Atlantic also influences rainfall variability (Reason *et al*., 2006). Inter-decadal variability has been previously linked to SSTs (Nicholson, 2000), evidence of this connection is presented in Reason and Rouault (2005) for the tropical southeast Atlantic and boreal summer rainfall over coastal West Africa and over southern Africa in summer related to ENSO-like decadal SST patterns (Reason and Rouault, 2002). However, it is suggested in Nicholson (2000) that SSTs may only result in a background state that can favour positive or negative rainfall anomalies therefore it cannot be concluded that SSTs force decadal rainfall variability over Africa. In the austral winter, the South Atlantic Ocean is a strong moisture source for both the West African monsoon and for westerly disturbances moving toward southern South Africa (Nicholson, 2000). The South Atlantic has also been proven to influence severe summer droughts over northern South Africa through advection of cool, dry air over South Africa as a result of a cyclonic anomaly being located over the southeast Atlantic (Mulenga *et al*., 2003).

### *1.4. The role of local topography*

Another factor that has important consequences for rainfall is the regional topography. Regions with steep topography such as the Drakensberg (**Figure 3**) in eastern South Africa, experience enhanced rainfall due to uplift of moist marine air masses advecting toward the topography (Reason, 2017). Garstang *et al.* (1987) indicated that interactions between westerly waves propagating across the southern tip of Africa and the topography of the north-eastern escarpment assist in the development of convective storms in the region. Circulation around the Angola Low and the interaction with local topography is thought to create favourable conditions for precipitation in the region (Cook *et al*., 2004). Over Madagascar, flattening of topography resulted in a weak MCT (Barimalala *et al*., 2018). There is also evidence that topography influences the spatial distribution of rainfall during the lifecycle of a COL (Abba Omar and Abiodun, 2021). However, the timing of peaks in rainfall do not seem to be influenced. Additionally, during a COL event the western topography further enhances rainfall, while the opposite is true over the eastern subcontinent (Abba Omar and Abiodun, 2021).

### *1.5. Large-scale rainfall producers over southern Africa*

As alluded to previously, rainfall over most of subtropical southern Africa occurs mainly in the summer. Heavy rainfall contributes a large fraction of the seasonal total and occurs during relatively short-lived events (Fauchereau *et al*., 2009, Roy and Rouault, 2013) typically driven by tropical-extratropical interaction and associated cloud bands. These cloud bands result from tropical extra-tropical interactions (Hart *et al*., 2010) between a midlatitude disturbance and tropical convection over the SWIO region. They extend northwest-southeast from the landmass to the adjacent Southwest Indian Ocean direction (Fauchereau *et al*., 2009). According to Macron *et al*. (2014), a systematic association between tropical extra-tropical temperature troughs (TTT) and a transient perturbation, interpretable as an atmospheric Rossby wave, was apparent. The reverse was not true, indicating that temperate perturbations alone are not sufficient for TTT development. The importance of planetary waves for TTT development is well demonstrated in Hart *et al*. (2010). It has also been previously indicated that a TTT coincides with moisture convergence over southern Africa (Todd and Washington, 1999, Todd *et al*., 2004, Fauchereau *et al*., 2009), this is caused by a reinforcement of the Angola low that favours flux penetration from the Atlantic region toward western southern Africa, and easterly moisture fluxes from the nearby Indian Ocean and the Mozambique Channel on the east (Macron *et al*., 2014). Strong rainfall anomalies and sea surface temperatures in SWIO, south of Madagascar are observed when the TTT are located over the continent. For example, the heavy rainfall and flooding during 12 – 14 February 1996 over the summer rainfall region of South Africa as a result of a tropical moist cloud band present over the region (De Coning *et al*., 1998). Shifts in TTT location have been previously associated with the highest (lowest) dry spell frequencies during El Niño (La Niña) events (Usman and Reason, 2004); however, Macron *et al*. (2014) argued that the contribution of continental TTTs to South African rainfall was not clearly ENSO dependent.

Additional systems such as tropical cyclones (TC), cut-off lows (COL), tropical lows, and mesoscale convective systems (MCS) are associated with heavy rainfall episodes over southern Africa (Taljaard, 1986, Singleton and Reason, 2007, Klinman and Reason, 2008, Mavume *et al*., 2009, Blamey and Reason, 2012, 2013, Reason, 2017).

Tropical cyclones affecting southern Africa form in the Southwest Indian Ocean and are influenced by several factors such as regional sea-surface temperatures (SST) and upper ocean heat content (Klinman and Reason, 2008). According to Mavume *et al*. (2009), very few cyclones in the Southwest Indian Ocean (SWIO) are formed if climatological SSTs are below 28°C. Mean genesis SST for cyclones in the Mozambique Channel were 29.5°C, based on daily SSTs up to a week ahead of the cyclone. It was observed in Reason and Keibel (2004) that large-scale circulation anomalies play an important role in influencing tropical cyclone evolution. For example, two weeks before tropical cyclone Eline reached 90°E, positive geopotential height anomalies and divergence over the tropical South Indian Ocean were present. Intense tropical cyclones are more common towards the end of the January – March cyclone season (Mavume *et al*., 2009) and also appear more frequently in the eastern part of the SWIO. Tropical cyclones formed west of Madagascar do not pose a threat to Mozambique, unlike that formed east of the island (Klinman and Reason, 2008). In fact, a decrease in TC landfall during 1980 – 2007 was apparent when a total of 64 tropical cyclones made landfall; of these, only 16 made landfall over Mozambique (Mavume *et al*., 2009). There have been cases where atypical tropical cyclones have affected eastern southern Africa, one prominent example being tropical cyclone Favio. This system made landfall 22°S, on the coast of southern Mozambique and tracked north-westward impacting the Mozambique coast further equatorward (Klinman and Reason, 2008). Inland penetration of SWIO tropical cyclones is also influenced by surface and SST conditions as well as the current La Niña state (Reason and Keibel, 2004). La Niña events typically lead to warm SST anomalies in the subtropical SWIO (Klinman and Reason, 2008), given these findings, not only did TC Favio exhibit unusual tracks but also made landfall during an El Niño event which is highly unlikely. Tropical storms over southern Africa can sometimes be remnants of tropical cyclones that have made landfall over Mozambique (Reason, 2017). These synoptic events contribute to rainfall along the tropical edge of the subcontinent (Howard *et al*., 2019). A large region of low pressure extending across Namibia to the South African coast was present after TC Eline merged with a heat low (Dyson and Van Heerden, 2002, Reason and Keibel, 2004). These tropical troughs can propagate eastward and cluster over Angola where they sometimes interact with TTTs (Howard *et al*., 2019) which was the case on February 29 and 1 March 2000 (Reason and Keibel, 2004).

A climatology of cut-off lows indicated that these systems accounted for a larger proportion of rainfall (i.e. total amount, frequency of rainy and extreme rainy days) along the south and east coast (Favre *et al*., 2013). Over South Africa, an extreme rainfall day occurring outside of the rainy season is often due to a COL as they are most common in the transition seasons (Singleton and Reason, 2007). Favre *et al*. (2013) also found that precipitation from COLs tends to be widespread and more intense in spring (October–December), making it the season of the strongest contribution of COL to annual precipitation over the country. The seasonality of their frequency varies regionally: in summer, they tend to be more numerous over the eastern Indian Ocean while in winter, they are more numerous over the Atlantic Ocean (Favre *et al*., 2013).

MCS also have maximum activity in the early summer, between November and December (Blamey and Reason, 2012, Wiston and Mphale, 2019); however, this peak period is closely followed by another peak in February (Blamey and Reason, 2012). Most of these systems develop within 250 km of the African continent with approximately 5% forming over the open ocean (Laing and Fritsch, 1993). Previous studies (Laing and Fritsch, 1993, Blamey and Reason, 2009) have associated the eastern escarpment with the development of MCSs. Laing and Fritsch (2000) suggest that southern Africa has favourable conditions for the development of MCSs over land and according to (Blamey and Reason, 2012), these systems tend to cluster in preferred locations, particularly along the eastern coastline. For example, Blamey and Reason (2009) provide a detailed analysis of the large MCS that produced almost two-thirds of monthly rainfall total at some stations in eastern South Africa between 1998 and 2006. They further suggested that the downstream propagation of these systems across the warm Agulhas Current–Mozambique Channel region could be related to the formation of cloud bands.

### *Summary*

The review has highlighted the regional and global influences on southern African rainfall variability. General atmospheric circulation is thought to be largely influenced by the tropical rain-belt. The summer rainfall region, which is prone to extreme daily rainfall events, is highlighted as the major contributor to the total annual rainfall over South Africa. The important rainfall-bearing

systems over southern Africa are tropical extra-tropical cloud bands, mesoscale convective systems, tropical lows, cut-off lows, and occasionally tropical cyclones. Regional topography is thought to influence rainfall over eastern southern Africa, where proximity to the warm Agulhas Current System, MCT, and warm SST temperatures are important to the local climate. ENSO, SAM, and the SIOD are thought to have influences on rainfall response over the region. Although their interactions are not well understood, ENSO and SIOD opposing phases are thought to have a strong precipitation response over southern Africa while the positive SAM phase is often associated with more abundant daily rainfall over, especially over central South Africa

# Chapter 2 Data and Methods

Since this thesis deals with extreme precipitation events, a discussion of available rainfall data sets is presented first.

## *2.1. Rainfall dataset*

Maidment *et al*. (2014) suggested that inter-comparisons of all available data sets is essential to quantitatively assess rainfall patterns and trends over Africa. They further added that the scarcity of records from existing rain-gauge networks comparatively makes it a challenge to understand current rainfall climatology over Africa. The majority of the satellite products give global or near-global coverage, but few are tailored solely for Africa (Maidment *et al*., 2014). Recent developments such as the Tropical Rainfall Measuring Mission (TRMM) have records of less than 30 years of rainfall data and thus cannot yet be used to infer long-term variability, especially in southern Africa. There is also evidence that satellite rainfall products have challenges over mountainous and coastal regions (Dinku *et al*., 2018); for example, TRMM, which has a spatial resolution of 0.25˚, could not capture the coastal effect in a study done over West Africa which could have been due to rainfall from stratiform clouds (Nicholson *et al*., 2003). Satellite rainfall estimates such as the monthly Global Precipitation Climatology Project (GPCP) that go back to 1979 (around 20 years earlier than TRMM), suffer from coarse spatial 2.5$^{o}$ resolution (Dinku *et al*., 2018). TARCAT (Tropical Applications of Meteorology using SATellite and ground-based observations (TAMSAT) African Rainfall Climatology and Time series) data are more suitable for regional drought applications and less skilful in monitoring flood events due to their underestimation of convective rainfall (Toté *et al*., 2015).

However, developments such as the Climate Hazards Group InfraRed Precipitation with Station data (CHIRPS) merge multiple data including satellite imagery and gauge records to provide robust estimates of rainfall (Funk *et al*., 2015); they have a quasi-global coverage (50˚S – 50˚N) at a 0.05˚ resolution for the period 1981 to near present. Various studies have used CHIRPS in comparison with other products to investigate rainfall variability and evaluate their performance over East Africa (Toté *et al*., 2015, Dinku *et al*., 2018, Gebrechorkos *et al*., 2018) and the Eastern

Cape province of South Africa (Mahlalela *et al*., 2020). CHIRPS showed a high correlation with station data and lower regional biases, moreover, observed daily and dekadal rainfall was well represented by CHIRPS in most validation regions compared to other products (Gebrechorkos *et al*., 2018).

This study uses CHIRPS rainfall data to investigate daily precipitation extremes over the PM. This product is more suitable for the PM region as part of its development was to monitor deep convective rainfall, as well as drought conditions over regions with complex topography (Funk *et al*., 2015). Only rainfall totals within the boundaries of the PM (shaded polygon), which covers northern KwaZulu-Natal, part of Mpumalanga and most of eSwatini (**Figure 1**), were used.

### *2.2. Extreme rainfall events identification and ranking*

The detection and ranking of daily extreme rainfall events is performed using a method initially proposed by Hart and Grumm (2001) and modified by (Ramos *et al*., 2014, 2017) for the Iberian Peninsula. As alluded to previously, the study region often experiences heavy rainfall in the summer months, and this methods fits well into the study because it takes into account not only the precipitation intensity but also its spatial extent (i.e. the area affected by the event). Precipitation anomalies above two standard deviation (2STD), which corresponds approximately to the 95$^{th}$ percentile, are calculated for each day and each grid-point. For the extended summer season (October – March), only grid points with wet days were taken into account (here defined as a day receiving rainfall amounts above 1 mm day$^{-1}$). A 7-day running mean is applied to the 95$^{th}$ percentile for each grid point to smooth the daily mean and the noisy climatological time series. To calculate the anomalies ($N$) the smoothed 95$^{th}$ percentile ($\mu$) values are subtracted from daily rainfall totals as follows:

$$N = precip_{c,i,j} - \mu_{c,i,j} \quad (1)$$

Extreme events are ranked based on their rarity or magnitude ($R$) given by an index that is obtained after multiplying:

$$R = N X M \quad (2)$$

1. The percentage of grid points with anomalies ($N$) above a certain the 95$^{th}$ percentile by

2. The mean ($M$) values of these anomalies for all grid points with precipitation anomalies over the 95$^{th}$ percentile.

This ranking method is sensitive to the smoothing filter such that some events may appear in different rank order if a 21-day running mean (instead of a 7-day) is applied (Ramos *et al*., 2014); however, this does not significantly alter the days included in the top 50. Additionally, some events which had severe socio-economic impacts over the region may not appear in the top rank and vice versa, i.e. events with no known severe impacts may be ranked higher. This method has also been successfully applied in Rapolaki *et al*. (2019) for the Limpopo River Basin of southern Africa. Two thresholds were used to define rainy days following Rapolaki *et al*. (2019). Moderate rain days were defined as days measuring 10 mm of rain per day or more, and a heavy rain day was defined as one receiving at least 25 mm of rain.

### *2.3. Synoptic classification*

An important part of this study was to identify the rainfall-bearing systems which led to extreme rainfall over the KwaZulu Natal region. To achieve this, various products were used to subjectively identify the synoptic setting during the time of each event. Gridded Satellite data (GridSat-B1) data, synoptic weather charts from the South African Weather Service, and NCEP/NCAR reanalysis data (Knapp *et al*., 2011, Kalnay *et al*., 1996) were used to identify different systems, including mesoscale convective systems (MCSs) and cut-off lows (COL). In addition to these products, the output from Hart *et al*. (2012) was used to identify tropical-extratropical cloud bands and the International Best Track Archive for Climate Stewardship (IBTrACS) data (Knapp *et al*., 2010) were used to identify tropical lows and tropical cyclones.

### *2.4. Modes of climate variability*

The relationship between the number of events and seasonal rainfall anomalies is investigated using standardized precipitation anomalies for the early (October–December, OND), late (January–March, JFM) and extended summer (October–March). Standardized precipitation anomalies are defined as:

$$X_i = \frac{P_i - \bar{P}_i}{\sigma_i} \quad (3)$$

Where $P_i$ represents the seasonal rainfall; $\bar{P}_m$ is the seasonal rainfall mean, covering the 1981–2018 period for the whole region, and $\sigma_i$ is the standard deviation of the seasonal rainfall totals for the same period in the region.

Potential links between some of the important climate modes and extreme rainfall events over the KwaZulu Natal region are assessed using correlation analysis with ENSO, SIOD, and SAM indices. The Niño 3.4 index used in this study is based on the Group for High Resolution Sea Surface Temperature (GHRSST) anomalies in the Niño 3.4 box (190°E–240°E; 5°S–5°N). The seasonal averages in the Niño 3.4 SST index below (above) -0.5°C (0.5°C) are defined as La Niña (El Niño), while the averages between -0.5 and 0.5°C are defined as neutral. For the SIOD, the index of Behera and Yamagata (2001) was used which is defined as the difference in SST anomalies between the eastern Indian Ocean (90°E–100°E; 28°S–18°N) and the southwestern Indian Ocean (55°E–65°E; 37°S–27°S). This study uses the SAM index of Marshall (2003), which is the monthly mean difference between the mean sea level pressure (SLP) anomalies at six stations close to 40°S and six stations close to 65°S.

### *2.5. Atmospheric circulation and SST*

In this study, the ERA-5 reanalysis data of the European Center for Medium-Range Weather Forecasts (ECMWF) at a resolution of 0.25 ° × 0.25° were used to examine circulation patterns

associated with the events. These data are available hourly from 1979 to near present; however, only monthly ERA-5 data are used here. Moisture fluxes at a particular level were computed from the product of the specific humidity and the wind at that level. To assess areas of relative uplift associated with the events, the 500 hPa vertical velocity was used. SST anomalies were assessed using the National Oceanic and Atmospheric Administration (NOAA) daily high-resolution-blended analyses which have a spatial grid resolution of 0.25° (Reynolds *et al*., 2007).

# Chapter 3 Results

## *3.1. Climatology*

**Figure 3** shows a topography map with the PM domain indicated by the red box, and the available SAWS rain gauge stations. The annual rainfall cycle averaged over the PM region using CHIRPS data is shown in **Figure 4**. Monthly mean rainfall more than doubles from September to October so the latter month could be regarded as the onset of the summer rainy season while March could be regarded as its end since the monthly mean halves from that month to the April mean. However, more sophisticated definitions of the onset and withdrawal dates use daily rainfall and are based on cumulative amounts (Dunning *et al*., 2018). Thus, defining the rainy season as October–March is an approximation that is convenient but may not be sufficiently accurate in some applications. On average, the rainfall peaks in January with a sharper decrease to the February mean than the increase from the mean December to the mean January value. May–August are relatively dry compared to the summer half of the year with the driest month being July on average. The observed annual cycle of rainfall is comparable with that found by Dube and Jury (2000) from 1964 to 1996 over northern KZN using the South African Weather Service data.

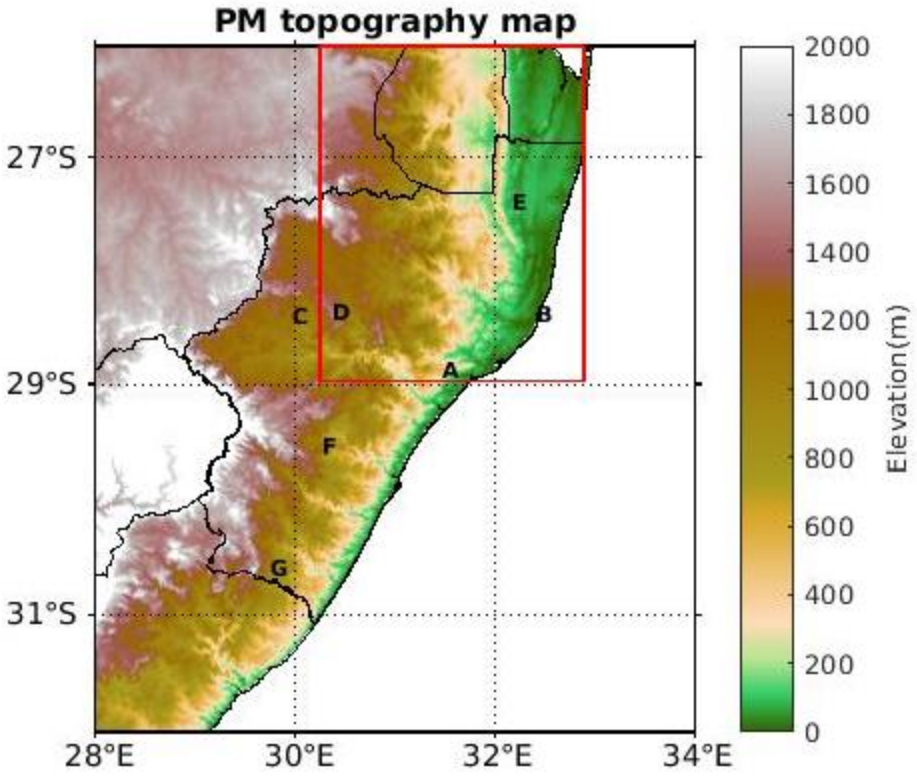


**Figure 3:** illustrates the topography (shaded; m) of the PM region along with the location of the SAWS stations in the area labeled A – G. The PM domain is shown as the red box. Produced with Global Land One-km Base Elevation Project (GLOBE) data.

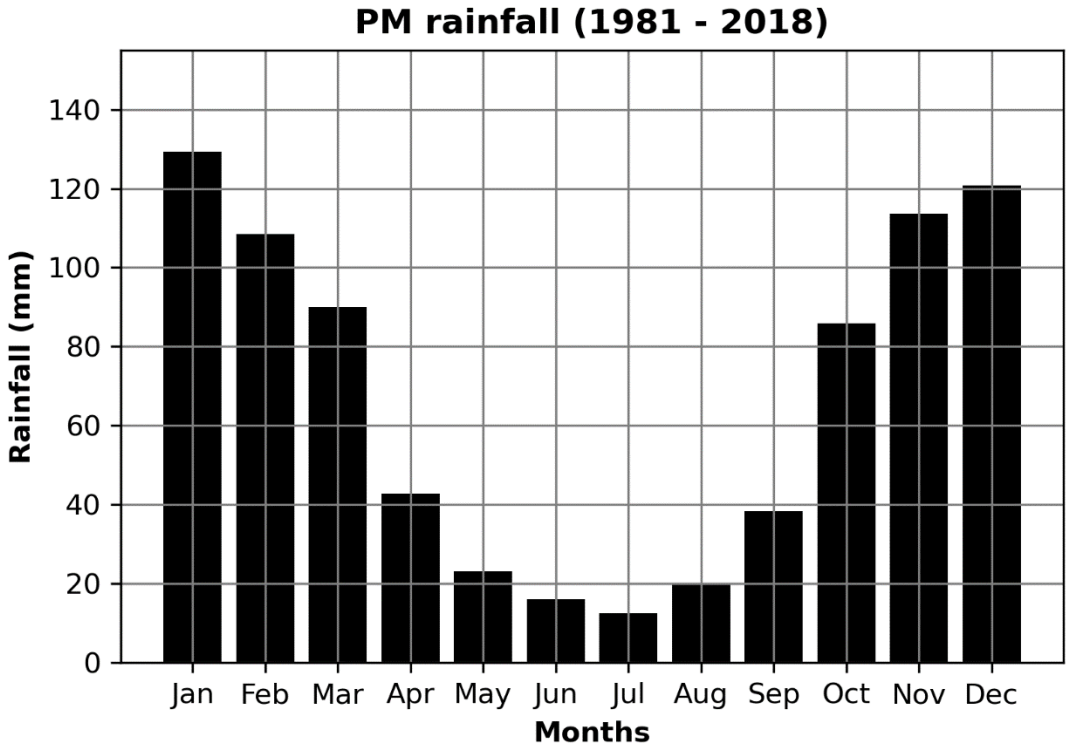


**Figure 4:** The annual cycle of rainfall over the northern PM domain in Fig. 2 (25.8° – 28.9° S to 30.2° – 32.8° E) for the period of 1981 – 2018. Produced with CHIRPS rainfall data.

Since **Figure 4** represents the spatially averaged annual cycle of rainfall across the PM region, it is of interest to determine whether there is any spatial variability in this seasonal cycle across the region. **Figure 5** plots the annual cycle of rainfall for eight South African Weather Service (SAWS) stations across KZN (see **Figure 3** for location). Of the five stations within the PM domain (**Figures 5a-g**), only two have a clear January peak (Eshowe and Swartwater) while St Lucia and Elandslaagte show a clear February peak and Makatini shows January only very slightly wetter than February. However, St Lucia shows a secondary peak in October giving it a bimodal character to its annual cycle to some extent. Cedara and Weza plantation which are both well south of the red domain respectively show December and January to have almost the same average rainfall and December to be clearly the wettest month. While all stations show a clearly wetter October–March summer half of the year relative to April–September, the drier winter is much less pronounced at the coastal station of St Lucia than at some inland stations such as Elandslaagte and

Swartwater. There are also small variations in the timing of the driest month with June being drier than July in a few cases. On average, St. Lucia (**Figure 5b**) receives the highest mean annual rainfall, consistent with Ndlovu *et al*. (2021), and suggesting proximity to the ocean and the warm Agulhas Current may play a role. There may also be topographic influences since inland station Makatini is drier than Swartwater and Elandslaagte which are further inland but closer to the Drakensberg Mountains. In fact, these two stations lie in the foothills of the Drakensberg where mean annual rainfall is strongly related to altitude and eastward distance from the escarpment (Nel and Sumner, 2006).

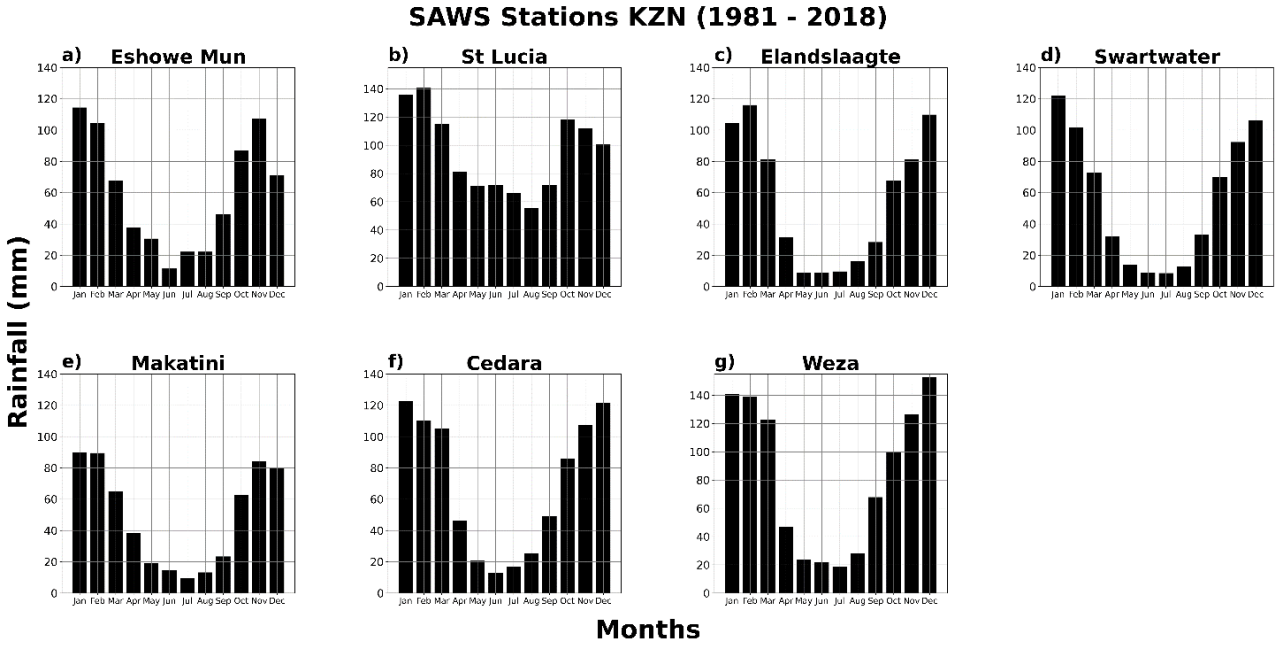


**Figure 5:** The annual cycle of rainfall over the various SAWS stations in KZN (**Fig. 3**) extending from the coast to further inland; (**a**) Eshowe municipality (**b**) St. Lucia (**c**) Elandslaagte (**d**) Swartwater (**e**) Makatini Research Center (**f**) Cedara (**g**) Weza Plantation. Produced with SAWS rainfall data from 1981 – 2018 for each station.

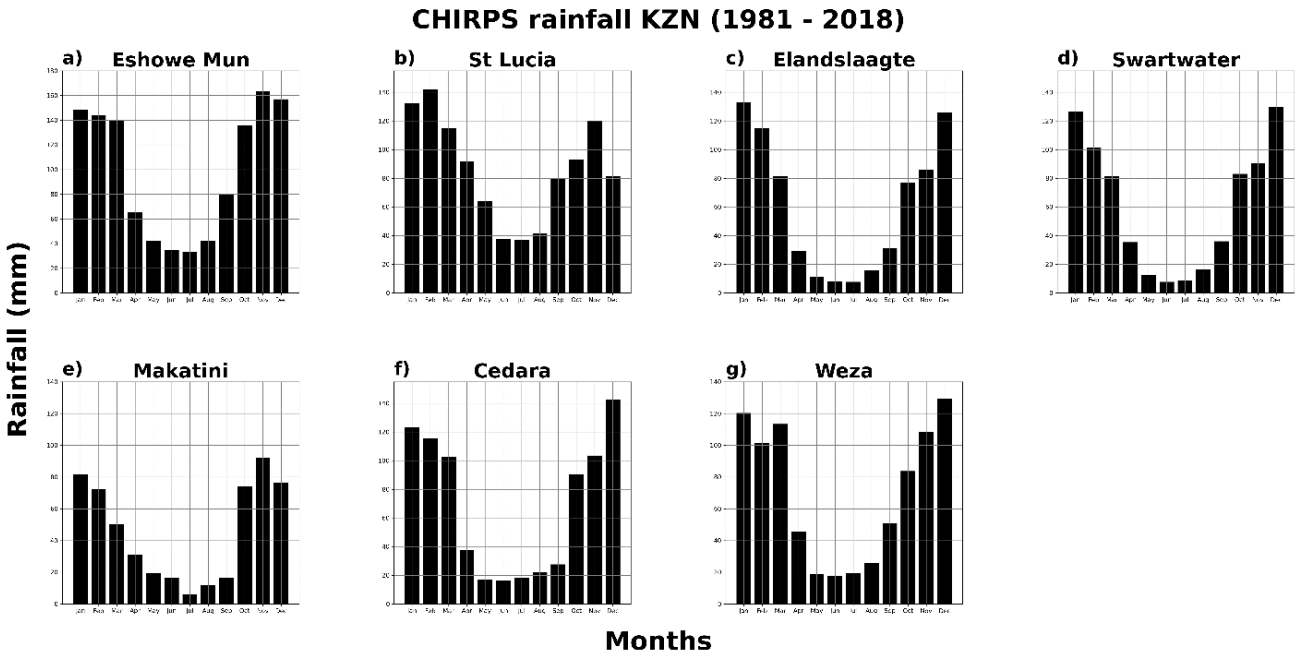


**Figure 6:** Same as **Fig. 5**, but for CHIRPS rainfall data.

To evaluate the satellite-derived CHIRPS data that is used in this study, a comparison is made with the stations from **Figure 5** with CHIRPS (**Figure 6**). Overall CHIRPS compares favourably well with the SAWS data. At four of these stations (Cedara, St Lucia, Swartwater and Weza) the wetter months are well captured by CHIRPS. For example at St Lucia, January – February are wetter with a clear peak in February and less pronounced dry winters compared to most stations (**Figure 6f–g**). The December peaks and wetter December – January months at the stations south of the domain (Cedara and Weza) are also clearly represented by CHIRPS. At Swartwater, there is also consistency in the wetter months; however, SAWS shows a clear peak in January whereas CHIRPS indicates almost the same average rainfall in December and January. For Elandslaagte (**Figure 6c**), the sharp increase from November to the December mean is comparable for both datasets with the CHIRPS January peak surpassing the SAWS February peak in gauge data. There is also a consistent sharp increase from the mean October to the mean November rainfall for Makatini (**Figure 6e**). The small variations in the timing of the driest month are less pronounced for

CHIRPS, June–July almost has the same lowest average for most stations except Makatini, where July is clearly the driest month for both datasets.

In summary, although there are spatial variations in the timing of the peaks of the average annual rainfall during the summer season across the region, both SAWS and CHIRPS show that December to February has the wettest overall average rainfall with June to July being much drier. The non-uniformity in the distribution of mean annual rainfall over the region is due to regional features such as the warm Agulhas Current System for stations near the coast, and orographic effects for stations with steep topography. In terms of the former, the strongest SST-rainfall relationships may exist with the northern part of the current, from 25˚to 30˚S (Walker, 1990) particularly where the continental shelf is narrow (Jury *et al*., 1993). The KZN inland regions generally have the lowest mean annual rainfall (Ndlovu *et al*., 2021), and this is well pronounced at the low-lying station of Makatini for both datasets.

### *3.2. Extreme weather events*

Using the methodology described in Section 2, the top 20 rainfall events and associated systems responsible for the heavy rainfall are presented in **Table 1**. This table shows that cut-off lows and tropical lows are the main contributors (7 and 6 out of 20 events, respectively) with the remaining 7 events more or less equally associated with cloud bands, MCS and tropical cyclones. Expanding the list to the top 50 events leads to tropical lows being by far the most common contributor (19 events), with MCSs, cut-off lows and cloud bands being associated with a similar number of events (10, 9 and 8 respectively) while tropical cyclones are associated with 4 events. However, note that the identification and ranking method used in this study is for daily precipitation extremes, and some events listed in the table can be linked to a synoptic weather system that was active on consecutive days. For example, the heavy rains on 29–31 January 1984 were linked to tropical cyclone Domoina.

**Table 1:** Shows the extreme daily rainfall events ranked in the top 20 over the PM region. The daily maximum rainfall total and associated synoptic weather type are also shown. Each event is ranked based on the areal extent of grid points that have rainfall anomalies above the 95$^{th}$ percentile of the long term climatology multiplied by the mean values of the anomalies over this percentage.

| Rank | Event | Rainfall (mm) | Synoptic weather type |
|---|---|---|---|
| 1 | 31-Jan-1984 | 247.3 | Tropical cyclone |
| 2 | 30-Jan-1984 | 174.1 | Tropical cyclone |
| 3 | 17-Mar-2000 | 202.1 | Tropical low |
| 4 | 23-Oct-1996 | 89.1 | Cut-off low |
| 5 | 22-Dec-1995 | 110.1 | Tropical low |
| 6 | 1-Jan-2000 | 135.4 | Tropical low |
| 7 | 11-Feb-1996 | 177 | Cloud band |
| 8 | 1-Jan-2001 | 95.9 | Cut-off low |
| 9 | 8-Mar-2016 | 186.4 | MCS |
| 10 | 5-Oct-1993 | 143.4 | Cut-off low |
| 11 | 6-Oct-1993 | 114.8 | Cut-off low |
| 12 | 18-Oct-1988 | 89.4 | Tropical low |
| 13 | 7-Feb-1985 | 151 | Cloud band |
| 14 | 24-Mar-1990 | 203.9 | Tropical low |
| 15 | 28-Nov-1989 | 97.3 | MCS |
| 16 | 17-Dec-2007 | 109.8 | Cloud band |
| 17 | 31-Oct-1985 | 162 | Cut-off low |
| 18 | 14-Oct-1994 | 100 | Cut-off low |
| 19 | 20-Nov-2009 | 97.3 | Cut-off low |
| 20 | 3-Mar-2012 | 191 | Tropical low |

**Figure 7** shows the spatial distribution of rainfall in the top 20 extreme events and synoptic weather systems linked with each event. Also shown is the maximum rainfall recorded on that day at any one grid point in the PM region. The maximum rainfall received during the top 20 events ranges from 89 mm (event #4) to 247 mm (event #1). High rainfall amounts often occur either where there are steep topographic gradients such as near the northern Drakensberg and Lebombo

mountains or near the coast, consistent with Nel and Sumner (2006). Muthoni *et al*. (2019) also found that rainfall maxima occurred near mountainous regions for long-term mean rainfall over eastern southern Africa. Over the PM domain shown in **Figure 3**, extreme rainfall linked to cut-off lows and tropical lows is mostly spread over a wider area than is the case for MCS and tends to penetrate further inland. However, an exception is event #14 which had the highest rainfall amount linked to tropical lows at any particular grid point but did not produce rainfall over a large land region. The tropical low (linked with event #20) also had maximum rainfall over the coastal areas of southern Mozambique and northeastern South Africa. According to Chikoore *et al*. (2015), the station of Charters Creek in northern KwaZulu Natal reported cumulative rainfall of more than 200 mm/day. As expected from their formation mechanisms and typical northwest to southeast orientation across subtropical southern Africa when they occur (Hart *et al*., 2013), the cases attributed to cloud bands also tend to show a diagonal rainfall distribution across the domain. The strongest cloud band case was event #7 in **Figure 7** and it caused flooding over many parts of the summer rainfall region of South Africa during 12–14 February 1996 (De Coning *et al*., 1998).

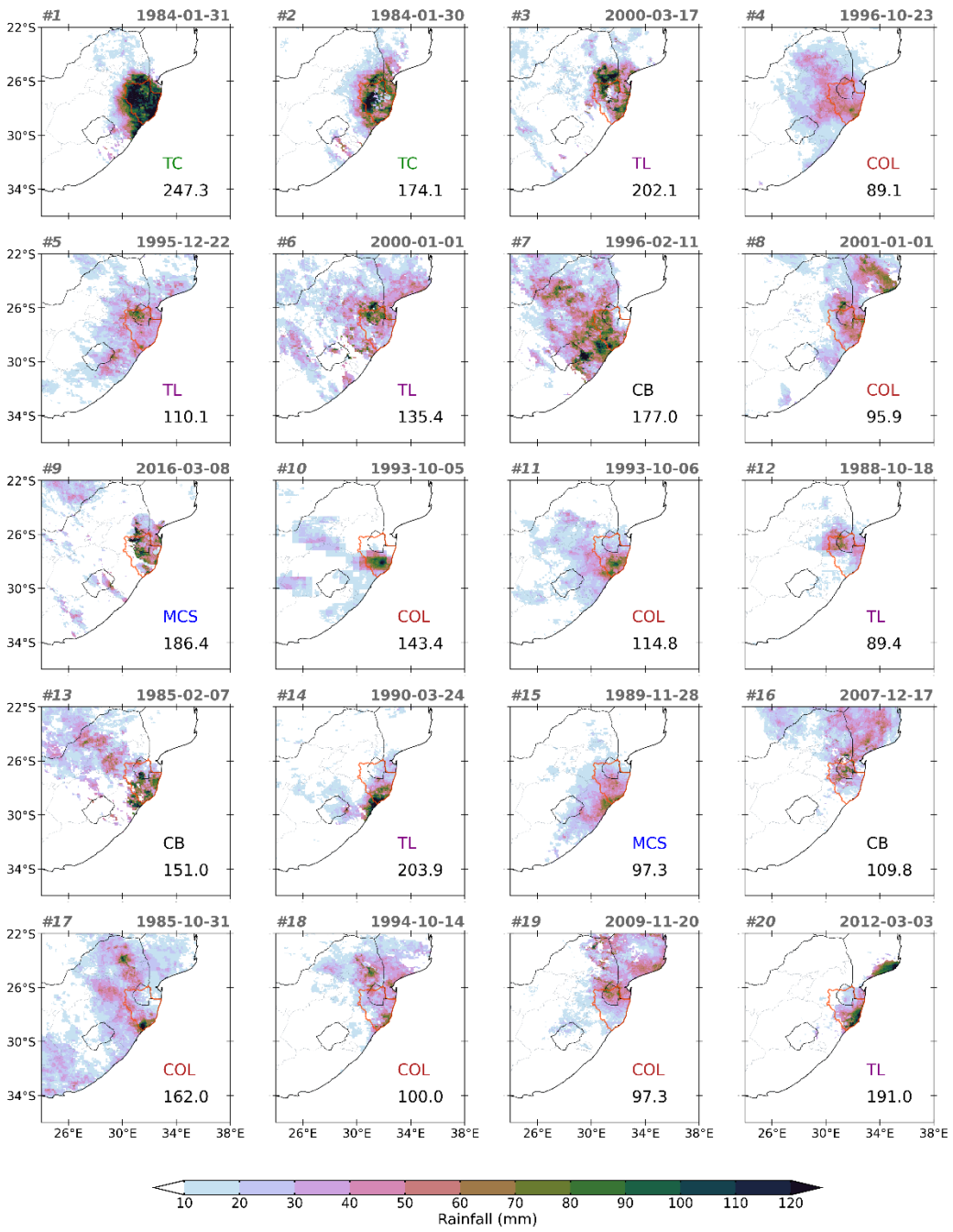


**Figure 7:** Spatial distribution of daily rainfall (shaded; mm) for extreme rainfall events ranked in the top 20 over the study region (pink polygon). Symbols CB, COL, MCS, TC and TL in the bottom right corner of each panel represent the different rainfall mechanism associated with each event (CB cloud band, COL cut-off low, MCS mesoscale convective system, TC tropical cyclone, TL tropical low). The maximum rainfall during each event is also shown in the bottom right corner.

For Tropical Cyclones, rainfall is confined to the coastal areas of the PM and southern Mozambique since most Tropical Cyclones making landfall on the southern Africa mainland tend to do so north of the domain (typically around 17–22$^{o}$S) and those in the southern Mozambique Channel tend to track well offshore from the southern Mozambique coast. An obvious exception was Tropical Cyclone Domoina (linked with the top ranked rainfall event in **Figure 7**) in late January 1984 which brought substantial rainfall as far inland as the Drakensberg.

### *3.3. Monthly frequency of the extreme events*

To create a more robust analysis, focus is now placed on the top 50 extreme daily rainfall events. The monthly distribution of the top 50 events in **Figure 8a** shows relative peaks in early summer (November) and late summer (March) with a relative minimum in December (half the number of the smaller November peak). This bimodal pattern contrasts with the annual cycle of rainfall spatially averaged over the PM which shows monthly totals increasing each month from the winter minimum to a peak in January after which the totals start to decrease (not shown).

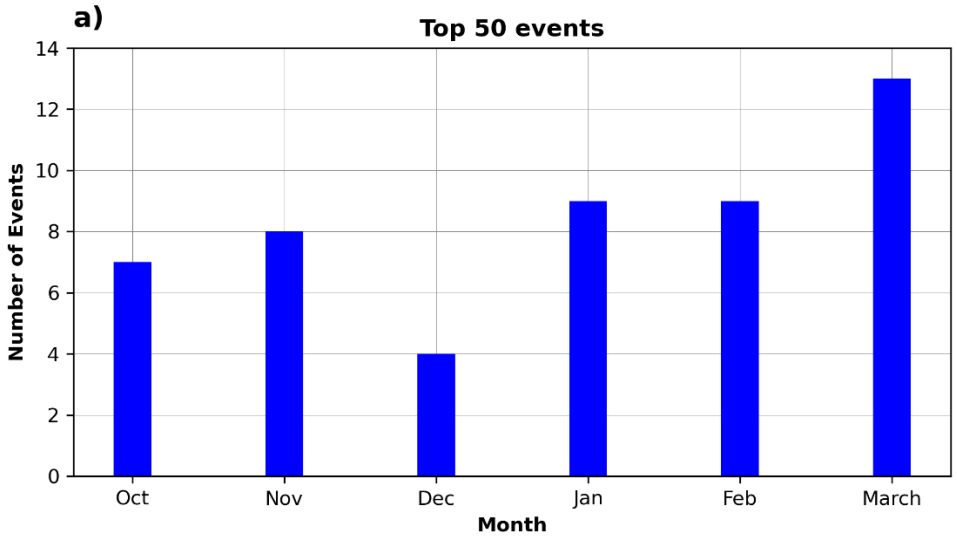

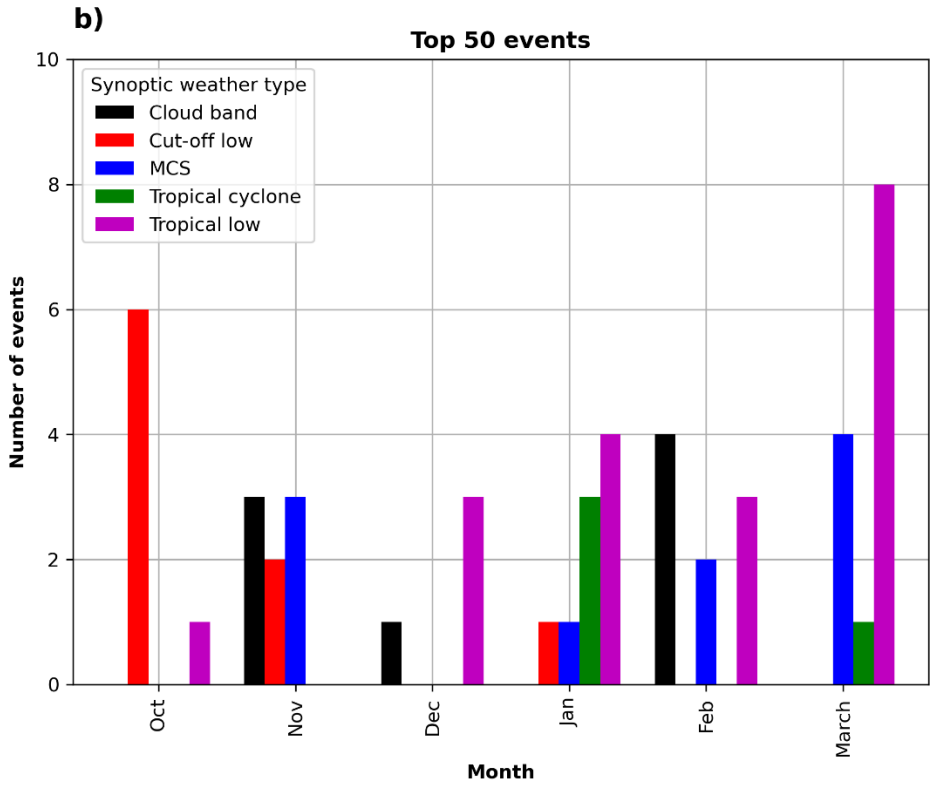


**Figure 8:** (**a**) The monthly distribution of the top 50 extreme rainfall events over the study region during October – March for the period 1981 – 2018. (**b**) Monthly distribution of the rainfall producing systems leading to extreme events over the region (cloud bands in black, COLs in red, MCS in blue, tropical cyclones in green and tropical lows in pink).

There is a sharp increase in the number of events after the minimum in December with the March maximum recording more than three times as many events as December during the period. While rainfall totals in March are less than all the other summer months except October, it is the month of maximum SST, which may favour tropical low development. Indeed, **Figure 8b** shows that more tropical lows occur in this month over the PM than any other month, consistent with what Rapolaki *et al*. (2019) found for the Limpopo River Basin. Only a few tropical cyclone cases have affected the PM; however, Mavume *et al*. (2009) found that intense tropical cyclones were more common later in the cyclone season (January–March). MCS numbers also peak in March with a weaker secondary peak in November. On the other hand cut-off lows peak in October and sharply decrease thereafter with none contributing in February and March. Cloud bands are more evenly

distributed throughout the season but with a peak in February and a weaker peak in November. This February peak in cloud bands is consistent with Hart *et al*. (2013) and Rapolaki *et al*. (2019) for South Africa as a whole and the LRB respectively.

### *3.4. Interannual variability of extreme rainfall events and relationships with large-scale climate modes*

Standardized rainfall anomalies for the PM and of the numbers of extreme rainfall events are compared for the early (OND; **Figure 9b**) and late (JFM; **Figure 9a**) summer, to help understand the potential impact of extreme rainfall events on the interannual variability of summer rainfall. There is substantial interannual variability in both OND and JFM rainfall totals as well as extreme events. However, as also observed in Rapolaki *et al*. (2019) for the Limpopo River Basin, the JFM seasons of anomalously low or high rainfall totals are not necessarily preceded by similarly dry or wet OND seasons suggesting that for the entire summer, the early and late summer anomalies may sometimes cancel out to some extent. For example, OND 1990 was somewhat dry whereas JFM 1991 was very wet and OND 2006 was very wet and JFM 2007 very dry. In terms of the relationship between the frequency of extreme events and rainfall anomalies, JFM 1984, 1985, 1988, 1991, 1996, and 2000 all experienced above average numbers of events as well as positive rainfall anomalies, JFM 2014 was relatively dry despite having two extreme events as compared to the average of slightly below 1(**Figure 9a**). For OND (**Figure 9b**), there are some wet seasons (1983, 1998, 1999, 2006) with no extreme events as well as 1994 which was dry and experienced an above average number of events. Although 1989 and 2000 which experienced well above average number of extreme events were also very wet seasons, there is not an obvious relationship between rainfall anomalies and the number of extreme events in OND. Thus, wet conditions, i.e. rainfall above one standard deviation, occurred during 3 out of the 12 OND seasons with extreme rainfall events. For JFM, there is a better correspondence with 6 out of 16 summers with above average number of events also experiencing wet conditions.

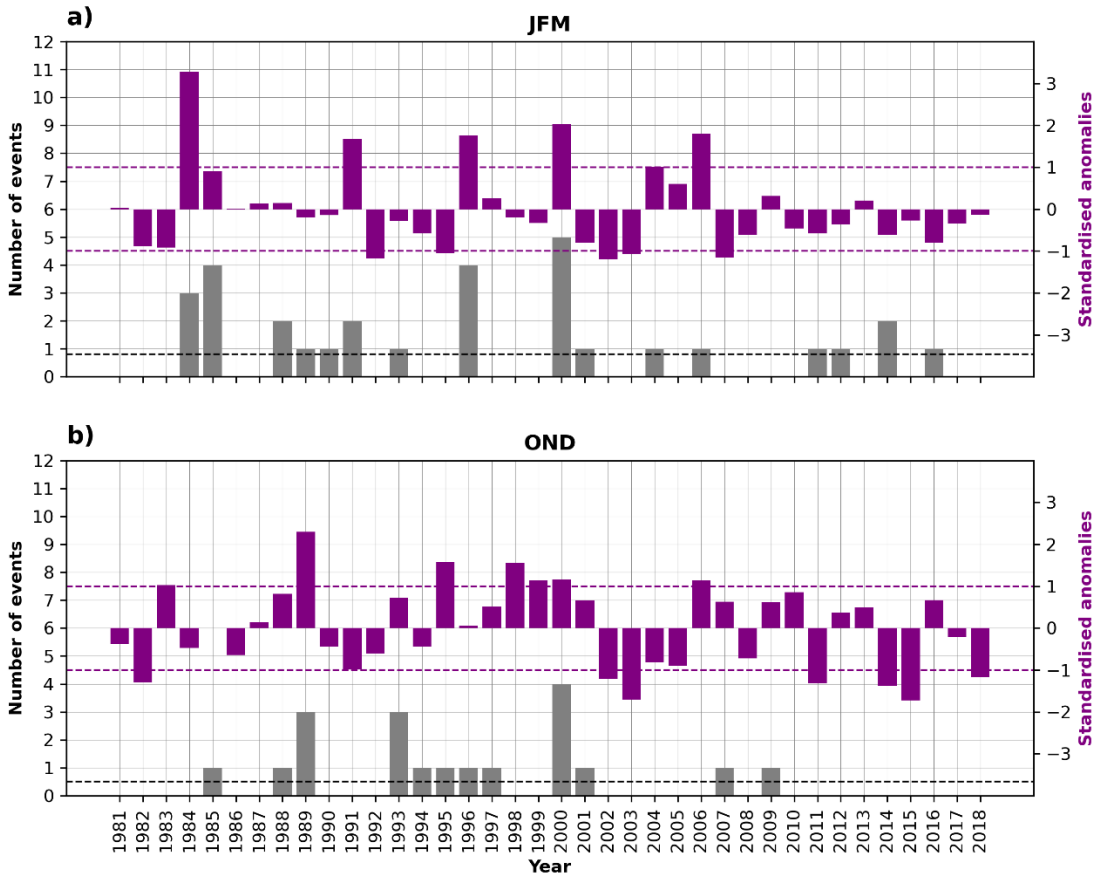


**Figure 9:** (**a**) Shows the standardized rainfall anomalies during the late summer season (January – March) in purple and the number of extreme events in the top 50 in grey for the period 1981 – 2018, (**b**) same as panel a but for early summer (October – December). Dashed purple lines in (**a**) and (**b**) are ± 1STD and the average number of extreme events are denoted by dashed black/grey lines.

The relationship between summer rainfall totals and the number of rainy days is examined for JFM (**Figure 10**) and OND (**Figure 11**). Rainy day frequency is determined by computing a percentage of grid points exceeding the respective thresholds within the study region. Two thresholds are chosen, one for days exceeding 10mm and the other for days exceeding 25 mm of rainfall. Days with at least 10% grid points exceeding each category of thresholds were selected for analysis.

JFM 1984, 1991, 1996, 2000, 2004, 2006 with strong positive rainfall anomalies (above one standard deviation (**Figure 10a)** tend to have increased rainy day frequencies (**Figure 10b**) and at

least one extreme rainfall event in each season (**Figure 10c**). Since ENSO typically impacts on southern African rainfall during JFM (Lindesay, 1988, Reason *et al*., 2000), it is of interest to consider potential relationships with this climate mode. Of these 6 JFM seasons, half were La Niña seasons but 1991 and 2004 were clearly neutral using the NOAA ONI (**Figure 10d**). Although 1984 is also marked as neutral in **Figure 10d**, the ONI is also indicative of La Niña in DJF (1983/84) and it only slightly fails to meet the La Niña criterion in JFM. Additionally, the strong MCT years (1982, 1984, 1989, 1994, and 2012) defined in Barimalala *et al*. (2020) all show JFM rainy days with above average numbers of 10 mm days and most show above average 25 mm days.

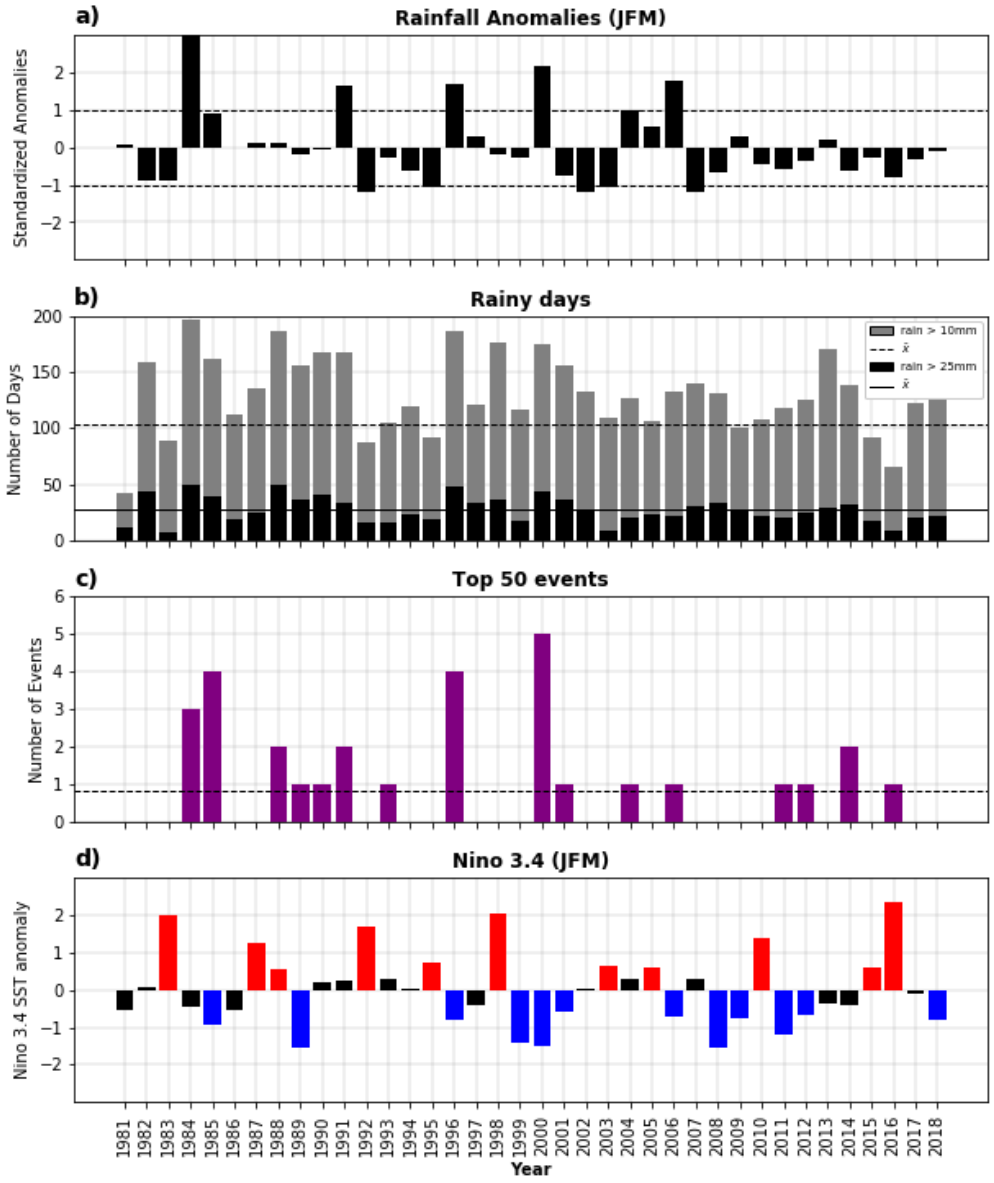


**Figure 10:** Comparison of (**a**) standardized rainfall anomalies over the study region from January to March. The dashed lines denote ±1STD. (**b**) number of rainfall days exceeding 10mm (25mm) for at least 10% grid points within the region in grey (black) bars. Dashed (solid) lines denote the mean for the respective thresholds. (**c**) The top 50 extreme rainfall events over the entire region during the period 1981 – 2018, with the dashed line showing the average number of events. (**d**) Nino3.4 index denoting the different phases of ENSO in red (El Niño), blue (La Niña) and black (neutral) bars.

For the JFM seasons with rainfall at least one standard deviation below average (1992, 1995, 2002, 2003, 2007) (**Figure 10a**), no extreme rainfall events (**Figure 10c**) occurred. However, of these five late summers, only 1992 and 1995 had below average number of rainy days (**Figure 10b**) while JFM 2003 had below average number of rainy days only for rain > 25 mm. Typically, El Niño is associated with below average rainfall over southern Africa and, of these five summers, only 2002 is clearly neutral while 2007 is El Niño in DJF (2006/07) but not quite in JFM 2007 (**Figure 10d**). The association with weak MCT years (1981, 1990, 2006, and 2017) is also not as good as wet JFM seasons, but 3 out of the set of 4 show below average 25 mm days.

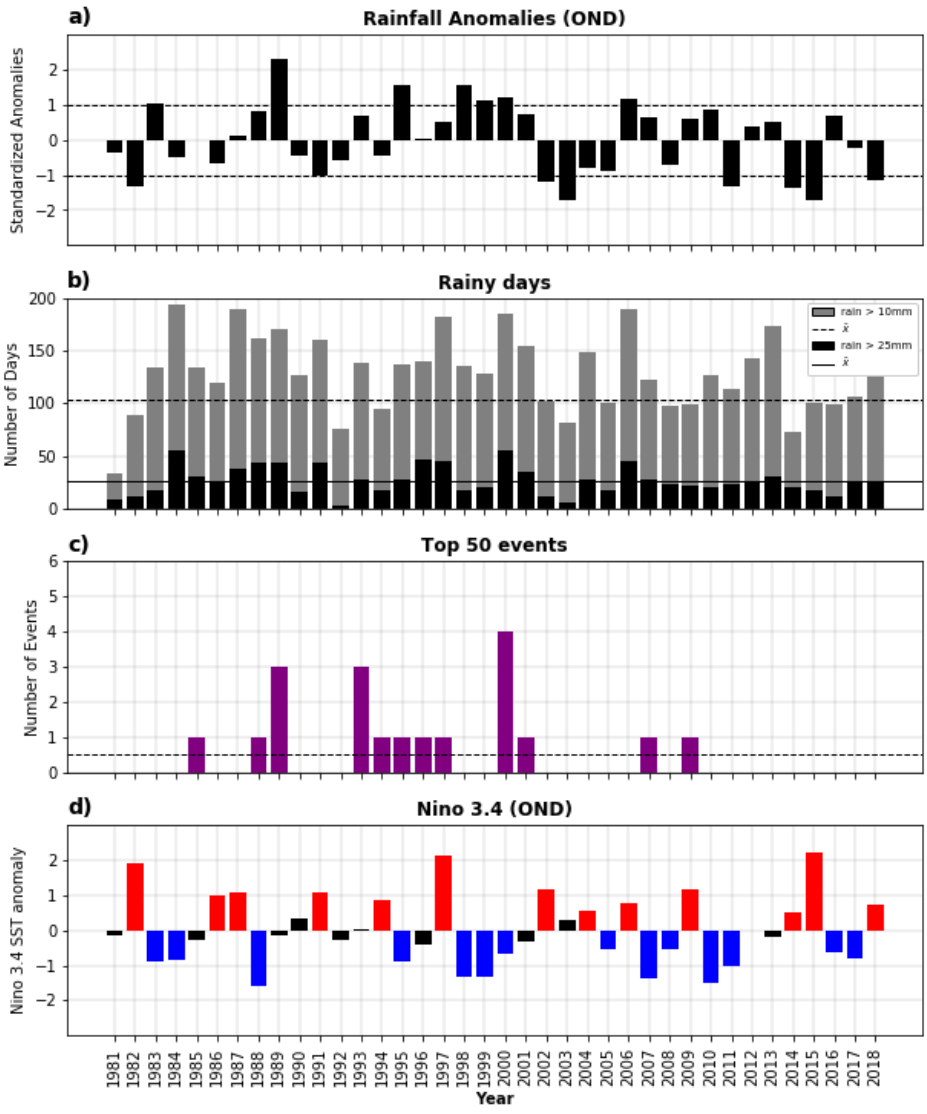


**Figure 11:** same as **Fig. 10**, but for OND.

OND seasons with strong positive rainfall anomalies (**Figure 11a**) (1983, 1989, 1995, 1998, 1999, 2000, 2006) also mainly had above average number of rainy days and several extreme events (**Figures 11b, c**). Exceptions are 1983, 1998 and 1999 all of which had below average number of days meeting the higher threshold > 25mm and no extreme events (**Figures 11b, c**). These results are consistent with the findings of Rapolaki *et al*. (2019) for the Limpopo River Basin where anomalously wet seasons were due to both an increased frequency and intensity of rainy days and extreme events. Most of these OND seasons correspond to a La Niña event (**Figure 11d**) but 1989 was neutral and 2006 experienced relatively strong El Niño conditions according to the ONI.

For dry OND seasons with at least one standard deviation below average rainfall anomalies (**Figure 11a**), the number of rainy days (**Figure 11b**) were below average for 1982, 2003, 2014 and 2015. On the other hand, OND 2004, 2011, 2018 had above average rainy days (rain > 10 mm). Zero extreme events were recorded during these dry OND seasons (**Figure 11c**). The strong negative rainfall anomalies during the early summers of 1982, 2004, 2014, 2015 and 2018 occurred during El Niño events, whereas 2003 was neutral and 2011 was La Niña. This anomalous 2011 season as well as OND 2006, which was El Niño but experienced wet conditions with well above average numbers of rainy days (both thresholds) and therefore also unexpected from the general ENSO-rain relationships, are analysed in terms of their circulation anomalies to establish why these rainfall anomalies may have occurred. Furthermore, a better understanding of circulation anomalies during ENSO events which have unexpected rainfall impacts is important because such improved knowledge will assist with climate diagnostics and with developing more accurate seasonal prediction tools for the region.

### *3.5. Circulation anomalies for 2006 and 2011 with atypical ENSO impacts*

Although ENSO has a statistically significant relationship with seasonal rainfall totals over the PM, particularly in JFM, the unexpectedly wet OND 2006 and dry OND 2011 suggest that other factors may have been important during these two seasons. Circulation anomalies during these two OND seasons are now considered.

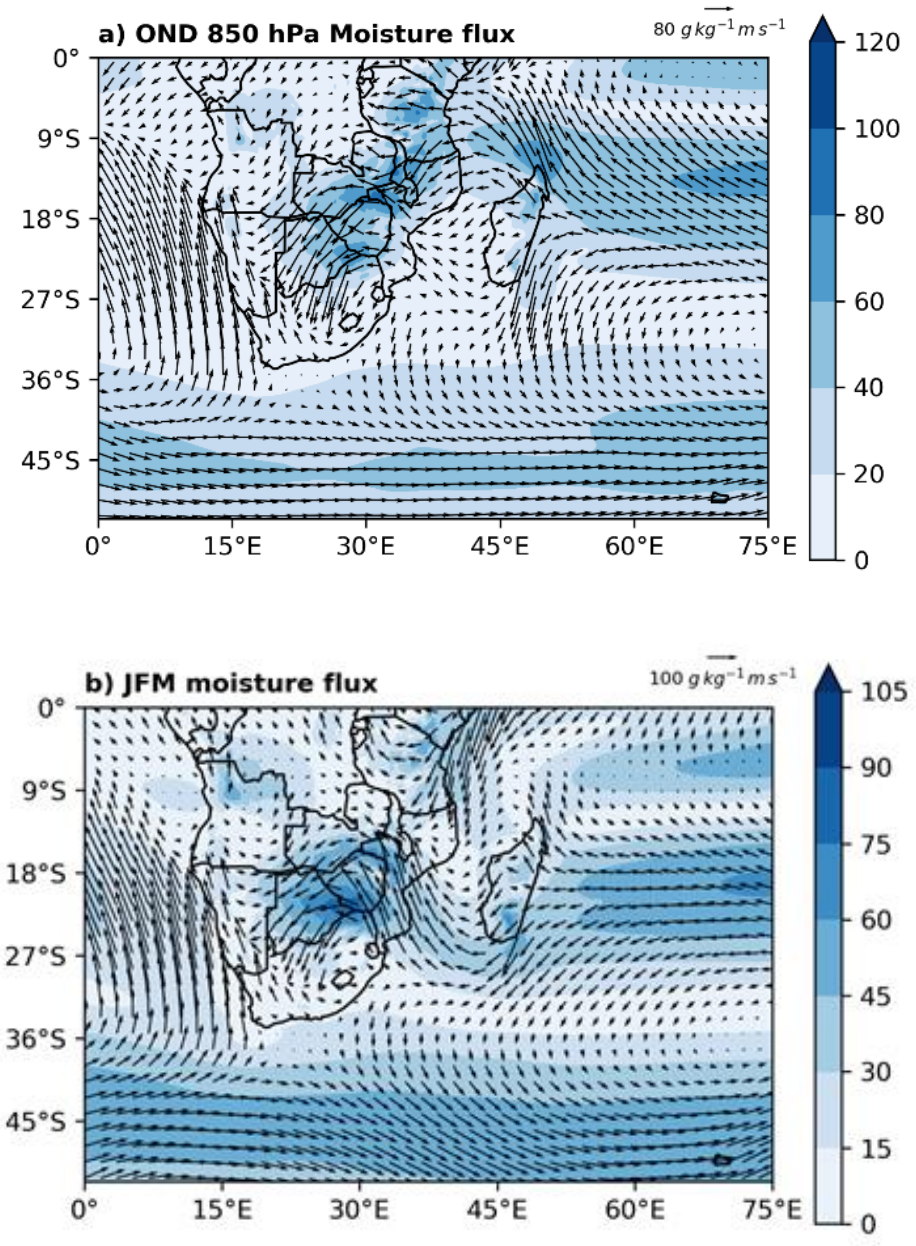


**Figure 12:** Climatology of low-level (850 hPa) moisture flux (shaded with vectors; g/kg $m^{-1}s^{-1}$) based on ERA-5 data for the period 1981 – 2018 for (**a**) OND and (**b**) JFM.

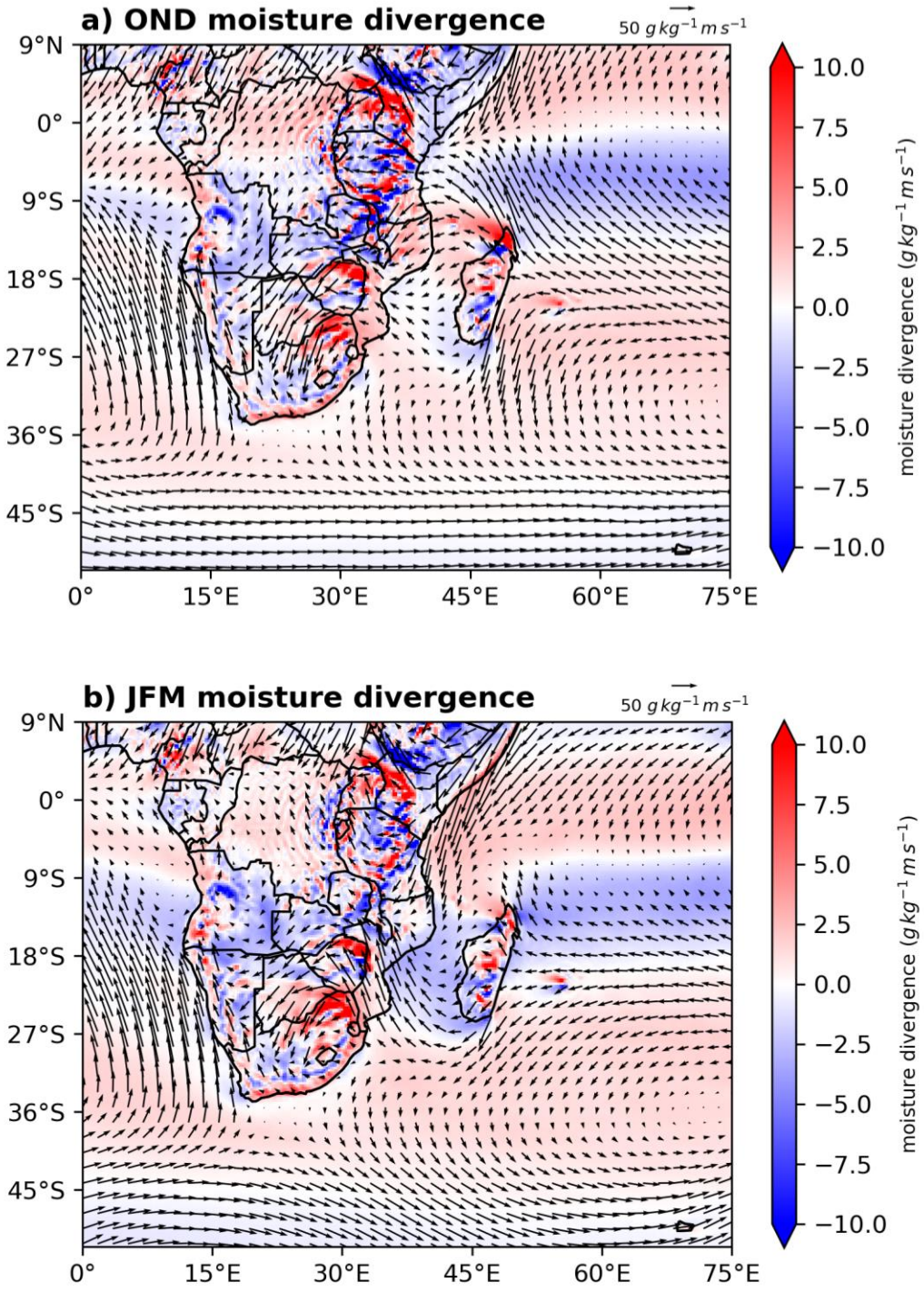


**Figure 13:** Climatology of low-level (850 hPa) moisture divergence (shading; g/kg $m^{-1}s^{-1}$) and moisture flux (vectors; barb in upper-right corner of plots shows scale) based on ERA-5 data for the period 1981 – 2018 for (**a**) OND and (**b**) JFM.

**Figure 12a** shows OND climatological moisture flux at the 850 hPa level and **Figure 12b** for the corresponding field for JFM. The moisture divergence is shown in **Figure 13a-b** for OND and JFM, respectively. During OND, there is strong easterly flux east of Madagascar which enters northern Mozambique and southern Tanzania as a northeasterly (NE) after crossing the northern Mozambique Channel. In the southern Channel, a weak cyclonic feature is apparent, reflecting the onset of the MCT (Barimalala *et al*., 2020), which feeds into a weak southeasterly flux over southern Mozambique. These circulation features in the south strengthen considerably in JFM with convergence over Zimbabwe and central to southern Mozambique. Further north, JFM shows a strong NE monsoonal flow over the tropical western Indian Ocean and the East African coast extending to northern Mozambique. **Figure 12b** also shows strong anticyclonic circulation of low-level moisture flux over eastern South Africa which is important during the development of heavy-rainfall producing systems such as cloud bands and MCSs when other conditions are favourable. There is also noticeable low-level convergence during the late and early summer in the tropical rain-belt, which stretches across the SWIO (**Figure 13**). Note that this seasonal climatology in ERA-5 does not show an obvious contribution from the tropical South East Atlantic or the Angola Low unlike those derived from NCEP reanalyses (Cook *et al*., 2004, Driver *et al.*, 2019). However, the low-level convergence over the Angola region does increase slightly in JFM compared to OND. A more obvious increase in low-level moisture flux convergence from OND to JM occurs in the central and southern Mozambique Channel.

This area of low-level convergence reflects the MCT which is prominent in the ERA-5 derived moisture fluxes, particularly in the late summer. This trough forms as the easterly trade wind flow adjusts to the mountains running down the length of Madagascar (Barimalala *et al*., 2018) but is also sensitive to SST in the South West Indian Ocean. Summers with a strong (weak) trough tend to be drier (wetter) over the mainland and the reverse over Madagascar as less (more) moisture feeds into the mainland (Barimalala *et al*., 2020). The Angola Low, which often acts as the source of cloud bands which bring much of the summer rainfall over subtropical southern Africa (Harrison, 1984, Hart *et al*., 2013) also tends to be stronger when the MCT is weaker, favouring wetter conditions over the mainland. Prominent areas of low-level moisture flux divergence are evident in the semi-arid Limpopo River Basin and also in the Zambezi River Basin. The former is the core of a drought corridor across subtropical southern Africa in summer (Usman and Reason,

2004, Thoithi *et al*., 2021). Although the seasonal analyses presented in **Figures 12** and **13** clearly show the importance of the tropical western Indian Ocean and the South West Indian Ocean as moisture sources over subtropical southern Africa, Lagrangian analyses have highlighted other sources such as the Congo Basin, the tropical South East Atlantic and the midlatitude South Atlantic / Agulhas Current (Rapolaki *et al*., 2019).

Moisture flux anomalies during the relatively weak El Niño of OND 2006, which was anomalously wet with above average numbers of both categories of rain days, is now examined. Strong easterly moisture flux anomalies from the tropical western Indian Ocean (**Figure 14a**) acted to feed more moisture into northern Madagascar right across the northern Mozambique Channel towards northern Mozambique. Over southern Tanzania / far northern Mozambique, there were southwesterly anomalies opposing the climatological flux (**Figure 14a**), implying relative convergence there. Similarly, there are southerly moisture flux anomalies over northern South Africa, Botswana and Zimbabwe during OND 2006 (**Figure 14a**) that oppose the mean flux (**Figure 12a**). The relative low-level convergence evident near the KZN coast (**Figure 14a**), as well as the weaker convergence over the PM area was favourable for wetter conditions during this season. Comparing **Figure 14a** with the El Niño composite (**Figure 17a**) suggests that the main difference in OND 2006 was stronger southerly anomalies over northern South Africa and Botswana as well as the presence of easterly anomalies over northern Madagascar in the northern Mozambique Channel. The latter may have been particularly important for the development of wetter conditions since the Mozambique Channel and indeed the entire South West Indian Ocean experienced above average SST during OND 2006 (**Figure 16a**). Warm SST anomalies in this region have previously been highlighted as favourable for wetter summers over eastern and northern South Africa (Reason and Mulenga, 1999) and in the tendency for cloud bands to be located over the landmass rather than offshore (Fauchereau *et al*., 2009).

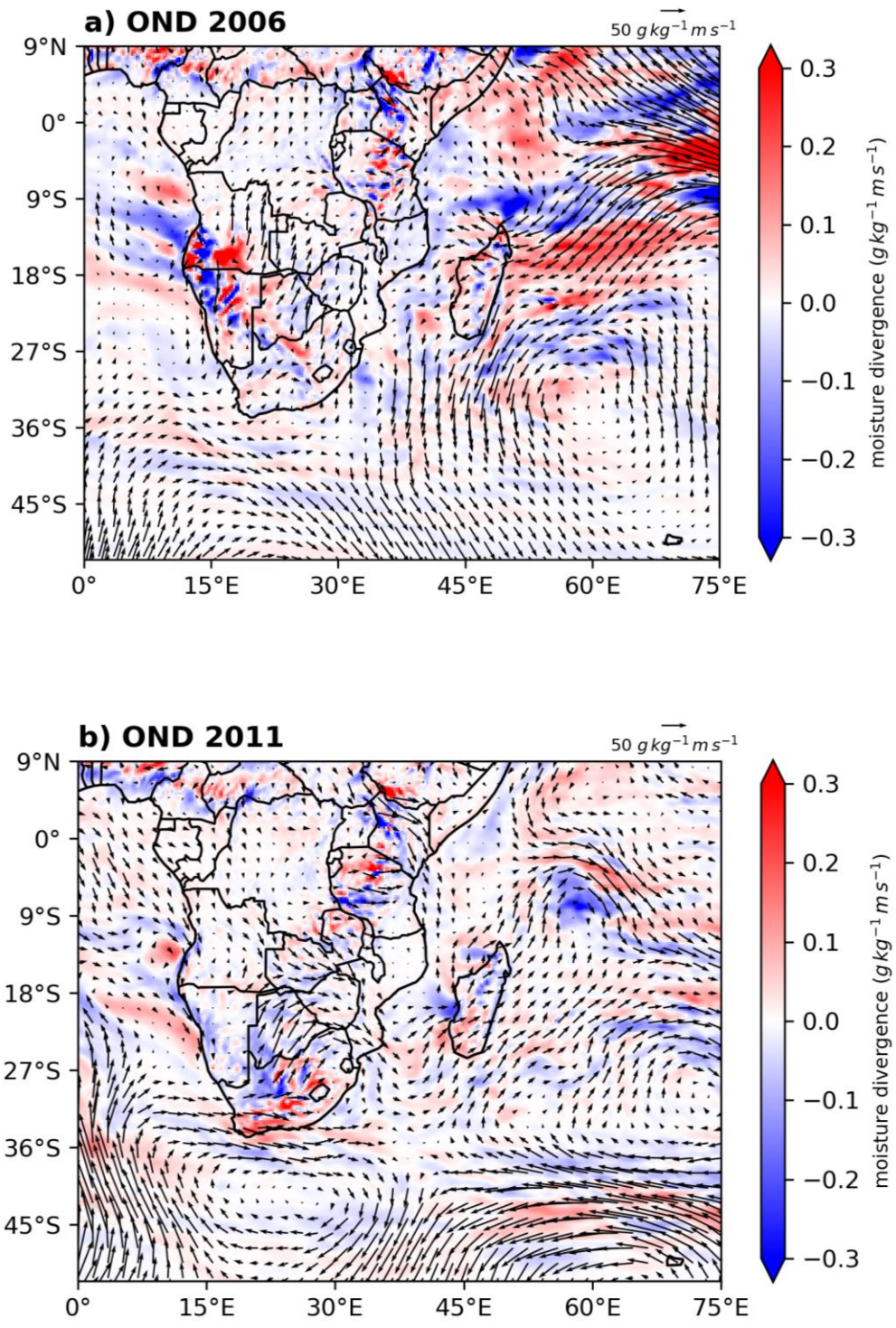


**Figure 14:** Low-level (850 hPa) moisture divergence (shading; g/kg $m^{-1}s^{-1}$) and moisture flux (vectors; barb in upper-right corner of plots shows scale) over southern Africa during OND for (**a**) 2006 and (**b**) 2011.

**Figure 15a** shows relatively strong uplift over most of northern South Africa including parts of the PM. The NW–SE orientation of these negative omega anomalies from southern Angola diagonally across subtropical southern Africa and out over the South West Indian Ocean suggests a cloud band type pattern. Further north, over the Mozambique Channel and central Mozambique there were positive anomalies suggesting less favourable conditions for convective rain-bearing systems developing well north and northeast of the PM. By comparison, the El Niño composite anomalies (**Figure 18a**) indicate positive anomalies (relative sinking) over the SWIO and most of southern Africa during this season. Over the PM, **Figure 11b** shows well above average numbers of heavy rainy days.

On the other hand, OND 2011 which experienced relatively strong La Niña conditions according to the ONI, received well below average rainfall (**Figure 11a**) although only the > 25 mm category of rain days was below average in number. Compared to the climatological moisture flux, **Figure 14b** shows a strong cyclonic anomaly south of South Africa which leads to westerly anomalies and low-level divergence over the southern half of South Africa. These types of anomalies imply a greater presence of cooler and dry South Atlantic air over the country associated with dry summers over northeastern South Africa (Mulenga *et al.*, 2003). The relative divergence evident over most of the PM area is consistent with drier conditions observed during this season. This cyclonic anomaly is much weaker and shifted to the southeast in the La Niña composite (**Figure 17b**) when wetter conditions are expected. Westerly anomalies are also apparent over Madagascar and much of the South Indian Ocean in OND 2011 implying less moisture flux from this source towards subtropical southern Africa. By contrast, the La Niña composite shows a stronger NE monsoonal flow over Tanzania and northern Mozambique as well as northerly anomalies over Zimbabwe and northern South Africa consistent with wetter conditions here in La Niña (Figure 17b). In OND 2011, the NE monsoon over Tanzania and northern Mozambique was not stronger; instead there were northwesterly anomalies over the adjacent ocean suggestive of relative diversion of moist NE monsoonal air away from the mainland and a reduction of the important moisture source for southern Africa of the tropical western Indian Ocean (Reason *et al.*, 2006, Rapolaki *et al.*, 2020) in this season.

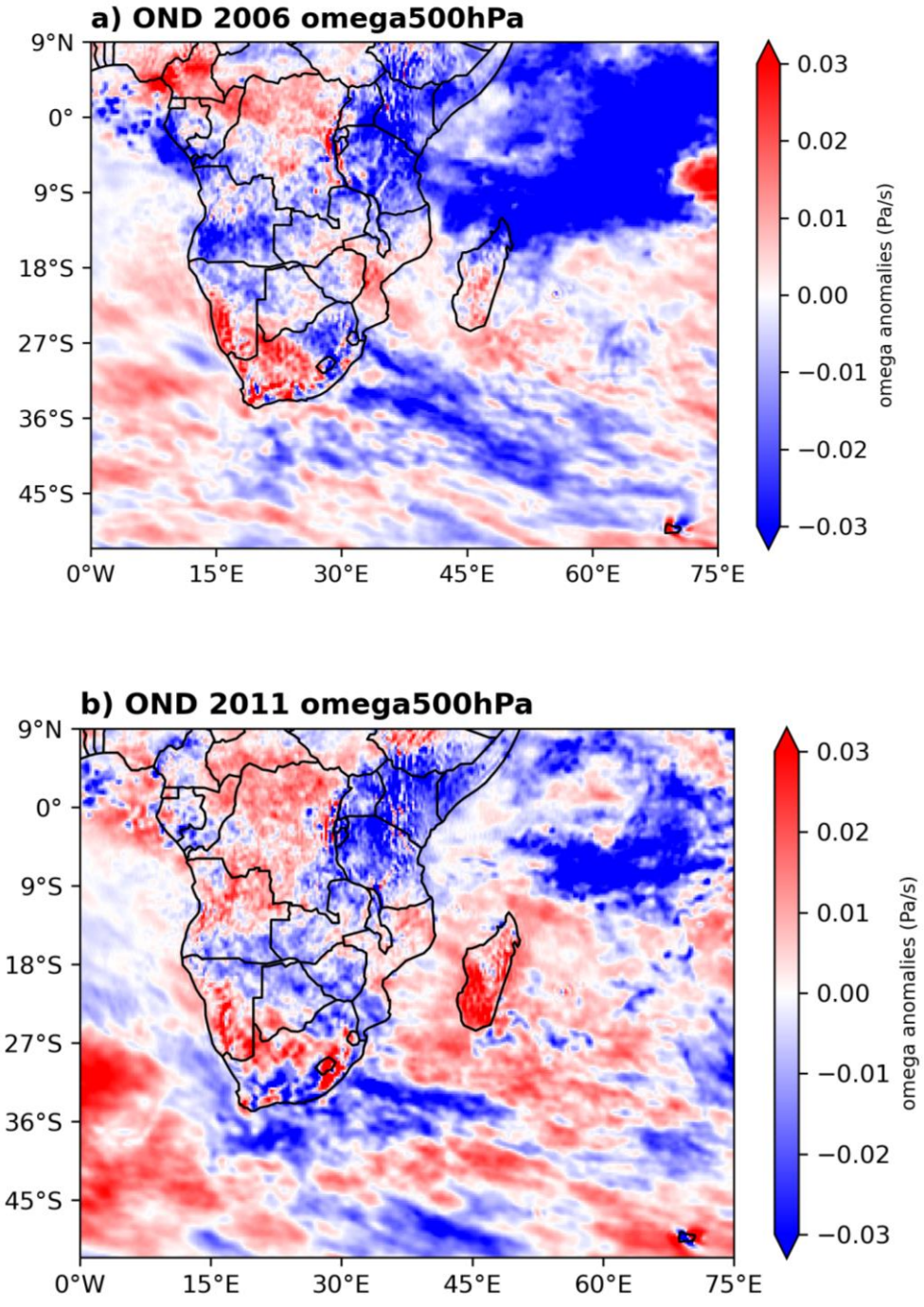


**Figure 15:** 500 hPa omega anomalies (shaded; Pa/s) over southern Africa during OND for (**a**) 2006 and (**b**) 2011.

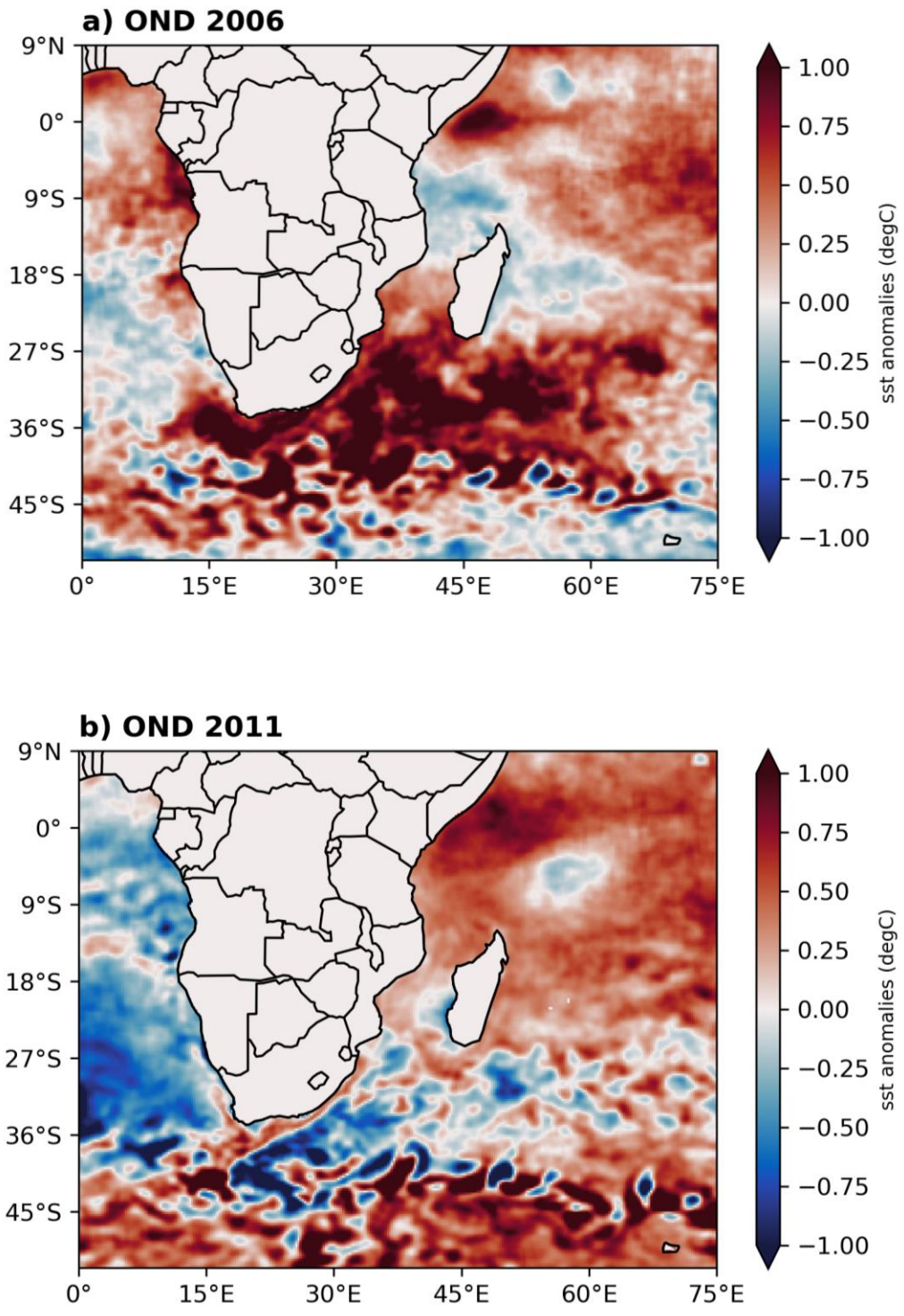


**Figure 16:** SST anomalies (shaded; °C) over southern Africa during OND for (**a**) 2006 and (**b**) 2011.

SST anomalies during OND 2011 (**Figure 16b**) were not as expected over the Indian Ocean during this phase of a La Niña event (Reason *et al*., 2000) since almost the entire basin showed warm anomalies. An exception was the Agulhas Current region which experienced cool SST anomalies, unfavourable for summer rainfall over northern and eastern South Africa (Mulenga *et al*., 2003). Although **Figure 15b** shows some areas of relative uplift near the coast of the PM area, much of eastern South Africa and the Mozambique Channel as well as the oceanic areas to its south show relatively strong positive omega anomalies. The positive anomalies (relative sinking) over eastern South Africa extend to the northwest (central northern Namibia) while there is a swath of negative anomalies further north. The strong positive omega anomalies are not apparent in the La Niña composite over much of southern Africa and the entire PM region (**Figure 18b**) which instead show large areas of negative anomalies (relative uplift) favourable for rainfall. These patterns suggest that in OND 2011 conditions for cloud bands may have been more favourable further north over Zimbabwe, Limpopo and southern – central Mozambique than the PM of interest.

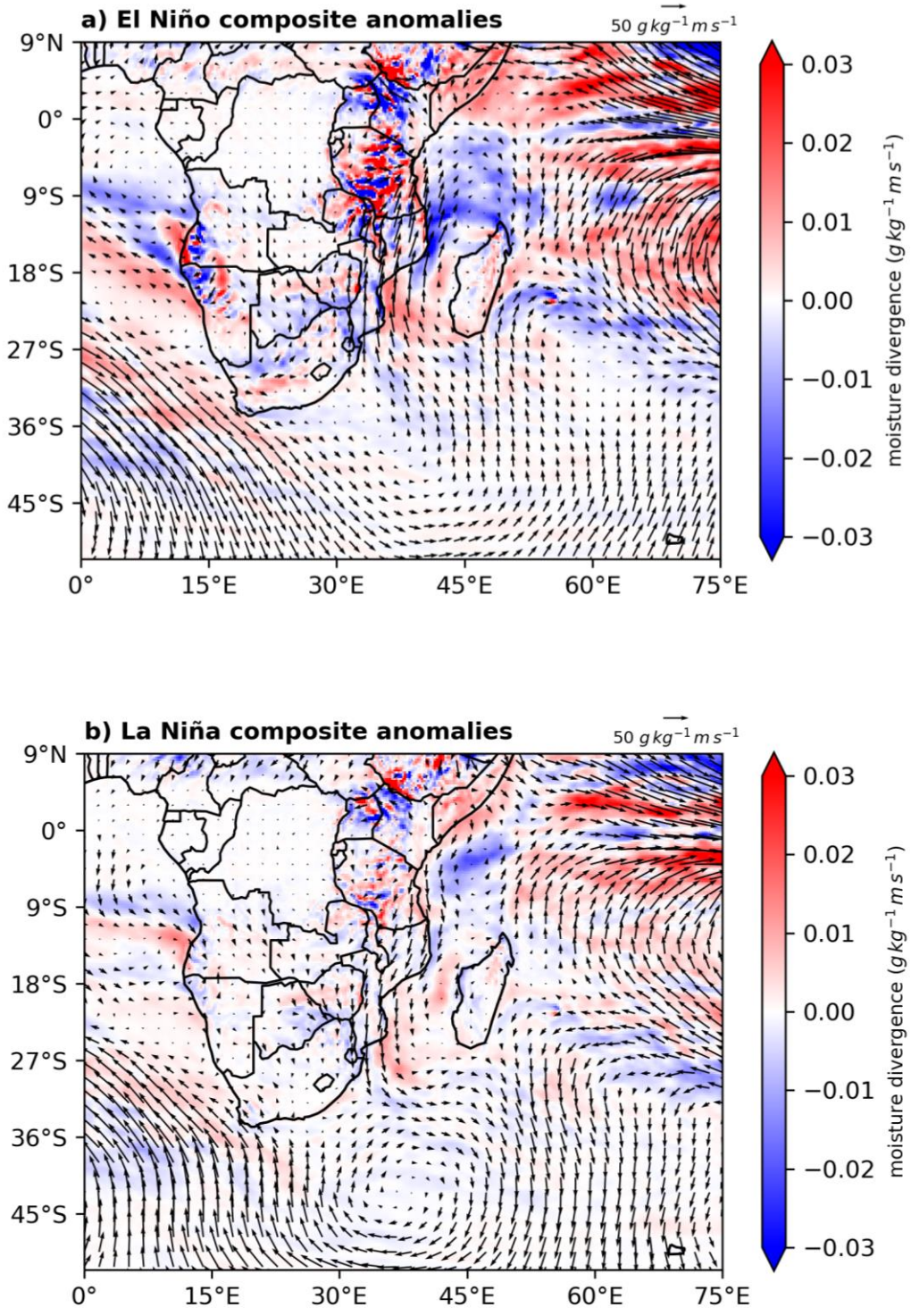


**Figure 17:** Composite anomalies of low-level (850 hPa) moisture flux (shaded with vectors; g/kg $m^{-1}s^{-1}$) over southern Africa during OND for (**a**) El Niño and (**b**) La Niña.

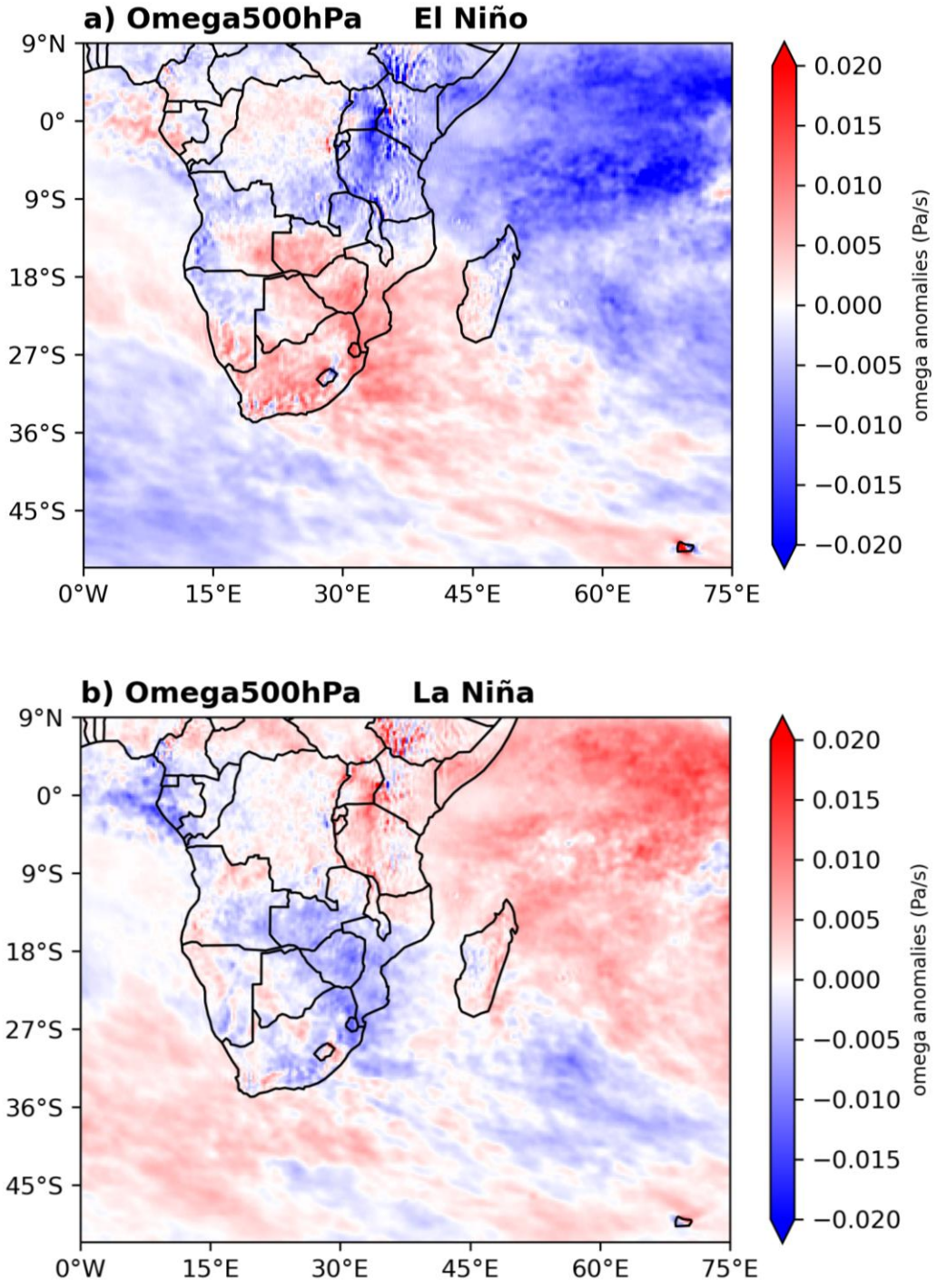


**Figure 18:** composite anomalies of 500 hPa omega (shaded; Pa/s) over southern Africa during OND for (**a**) El Niño and (**b**) La Niña.

# Chapter 4 Summary and conclusion

The objective of this study has been to investigate extreme daily rainfall events over the PM region and their associated synoptic weather systems. Given that this region receives the bulk of its rainfall during summer, and is prone to extreme climate conditions which sometimes have severe socio-economic impacts, the analysis has focussed on the extended summer season (October - March) for the period 1981 – 2018. Although there are still challenges regarding the identification and ranking of extreme rainfall events over southern Africa due to a lack of long-term gauge records and limitations in the satellite products over mountainous and coastal regions, the study has compared station observations and the CHIPRS rainfall product over the PM region to assess the mean annual rainfall.

The classification of the top 50 extreme rainfall events indicates that most events over the region are associated with tropical lows (40%) followed by MCS (20%), with the remaining 40% contributed to by cut-off lows, cloud bands, and tropical cyclones. The association of tropical lows with heavy rainfall over northern KwaZulu-Natal is in agreement with Harrison (1984). Cloud bands often make a greater contribution to heavy rainfall events elsewhere in the summer rainfall region of South Africa (Hart *et al*., 2010, 2013) or over the Limpopo River Basin (Rapolaki *et al*., 2019). An obvious difference with the latter is that the PM lies downstream of the mid-level westerly flow passing over the escarpment, and is also adjacent to the warm Agulhas Current. Such a setting has previously been suggested as favourable for MCC development compared to inland southern Africa (Blamey and Reason, 2012, 2013). Spatially, rainfall linked with extreme rainfall events is not uniformly distributed over the region. More extreme events occur in mountainous regions where orographic effects enhance extreme rainfall (Roy and Rouault, 2013), this is especially evident during mesoscale convective events (Blamey and Reason, 2009). Low-lying areas near the coast also tend to receive high rainfall amounts due to their proximity to the warm northern Agulhas Current as well as the southern Mozambique Channel where there is increased activity of tropical storms, including the occasional tropical cyclone.

The monthly distribution of extreme rainfall events showed that the late summer months (January – March) had the highest number of events in the top 50, consistent with Rapolaki *et al*. (2019)

over the Limpopo River Basin. Over 60% of extreme events occur during JFM, a season where intense tropical cyclones are most common (Mavume *et al*., 2009). In JFM, the numbers of tropical lows increases substantially to reach a maximum in March which has double the number in January. Cloud band and MCSs are distributed throughout the season with peaks in February and March, respectively. This February peak in cloud band systems is consistent with Hart *et al*. (2012) and Rapolaki *et al*. (2019). The maximum frequency for cut-off lows is October after which their frequency sharply declines with none contributing in February or March. Previous work (Singleton and Reason, 2007, Favre *et al*., 2012) showed that October and April were the months when cut-off lows were most common over South Africa.

On interannual time scales, the number of extreme events during JFM seasons was greater than in OND seasons. The latter were concentrated during 1988-2009 with no cases from 2010 onwards whereas the JFM events were more evenly distributed during the 1981-2018 period, albeit with clear maxima in the mid-1980s, 1996 and 2000. For OND, only 25% of the top 50 extreme rainfall events were associated with positive anomalies in rainfall totals whereas, for JFM, almost 40% of the seasons with extreme events also showed above average rainfall amounts. Both the intensity of daily rainfall and the number of heavy rainy days contributes to rainfall totals and in JFM there appears to be a more consistent contribution from both factors in leading to anomalous totals than in OND.

There is substantial evidence that ENSO influences rainfall totals over southern Africa (Lindesay, 1988, Reason *et al*., 2000, Nel and Sumner, 2006, Manhique *et al*., 2011, Blamey *et al*., 2018) as well as over KwaZulu-Natal (Ndlovu and Demlie, 2020). For the PM area, rainfall totals are correlated with the ONI at $r = -0.47$ in OND and $r = -0.33$ in JFM, both significant at 95%. The relationships between rainfall characteristics and ENSO over KwaZulu Natal and the PM as a whole, are not well understood. Correlating the frequency of extreme events over the PM with the ONI leads to a statistically significant result in both OND ($r= -0.47$, $p < 0.05$) and JFM ($r = -0.39$, $p < 0.05$), which are very similar values to those for the rainfall totals. The stronger correlations with the early summer rainfall are different to many other areas of southern Africa where JFM tends to show stronger correlations than OND. Other climate modes such as the Southern Annular Mode and the South Indian Ocean subtropical dipole gave mixed results. The latter did not show

significant correlations in either season and indeed the typically impacted region over southern Africa by this mode tends to lie further to the west and northwest (Behera and Yamagata, 2001) The Southern Annular Mode showed a significant positive correlation with extreme event frequency only in OND ($r = 0.40$, $p < 0.05$). Previous work by Gillett *et al*. (2006) showed evidence that this mode is positively correlated with summer rainfall over most of eastern and northern South Africa south of 25$^{o}$S which may result from anomalous easterly moisture transport from the South West Indian Ocean.

Although the ENSO signal was generally consistent in rainfall totals and heavy rain days over the PM, the anomalously wet OND 2006 season (El Niño) and dry OND 2011 (La Niña) were obvious exceptions. Analyses of moisture fluxes and omega fields during these two seasons suggested that enhanced easterly moisture transport over the northern Mozambique Channel, relative moisture flux convergence over much of eastern South Africa and a NW-SE band of enhanced uplift across subtropical southern Africa played a role in the former season being anomalously wet with substantially greater than average numbers of heavy rain days. On the other hand, the unexpectedly dry OND 2011 season seems to have resulted from westerly moisture flux anomalies over the southern half of South Africa (thereby favouring a drier, cooler South Atlantic air mass there) and strong westerly anomalies over much of the subtropical South Indian Ocean thereby reducing moisture inflow from this source. SST anomalies over the Indian Ocean were also unlike what typically occurs during La Niña seasons and also included cool anomalies in the Agulhas Current region, again unfavourable for rainfall over eastern and northern South Africa.

The results presented here suggest that the distribution of the mean annual rainfall over the PM region is influenced by regional features such as the warm Agulhas Current System and the topography with the highest rainfall amounts typically occurring in the coastal regions or near steep topography (Jury *et al*., 1993, Blamey and Reason, 2009). Tropical lows have been identified as the main contributors to extreme daily rainfall events over the PM and they are most common in March, albeit the location of cloud bands further north of the region can suppress rainfall in the PM while the opposite enhance conditions favourable for rainfall. On the interannual time scale, anomalously wet seasons do not always coincide with extreme daily rainfall events and vice versa. This suggests that for the rainy season (October – March), anomalous rainfall is due to the

frequency and intensity of rainy days as well as extreme daily rainfall events. ENSO-rainfall relationships over this region showed an overall significant result, especially during JFM. These relationships are well pronounced for wet seasons compared to dry seasons. However, some of the wet ENSO-neutral JFM seasons coincided with strong MCT years suggesting that easterly moisture transport from the Mozambique Channel region to the landmass may have otherwise resulted in these anomalously wet seasons.

This study has contributed a better understanding of extreme daily rainfall events over the PM area. Given the coastal location and steep topographic gradients of this region, the CHIRPS dataset may not be enough to accurately capture extreme daily rainfall near such regions (Dinku *et al.*, 2018). This suggests a need for more rain-gauges over the PM to help constrain satellite products to reality. The results provide a basis for potential work on daily rainfall extremes using model estimates in addition to the currently available data; this could help develop more accurate daily rainfall forecasts for the PM and similar regions.

# References


Abba Omar, S. & Abiodun, B. J. 2021. Simulating The Influence Of Topography On Cut-Off Lows Over Southern Africa. *International Journal Of Climatology,* 41**,** E2231-E2243.

Barimalala, R., Blamey, R. C., Desbiolles, F. & Reason, C. J. 2020. Variability In The Mozambique Channel Trough And Impacts On Southeast African Rainfall. *Journal Of Climate,* 33**,** 749-765.

Barimalala, R., Desbiolles, F., Blamey, R. C. & Reason, C. 2018. Madagascar Influence On The South Indian Ocean Convergence Zone, The Mozambique Channel Trough And Southern African Rainfall. *Geophysical Research Letters,* 45**,** 11,380-11,389.

Behera, S. K. & Yamagata, T. 2001. Subtropical Sst Dipole Events In The Southern Indian Ocean. *Geophysical Research Letters,* 28**,** 327-330.

Blamey, R., Kolusu, S., Mahlalela, P., Todd, M. & Reason, C. 2018. The Role Of Regional Circulation Features In Regulating El Niño Climate Impacts Over Southern Africa: A Comparison Of The 2015/2016 Drought With Previous Events. *International Journal Of Climatology,* 38**,** 4276-4295.

Blamey, R. & Reason, C. 2009. Numerical Simulation Of A Mesoscale Convective System Over The East Coast Of South Africa. *Tellus A: Dynamic Meteorology And Oceanography,* 61**,** 17-34.

Blamey, R. & Reason, C. 2013. The Role Of Mesoscale Convective Complexes In Southern Africa Summer Rainfall. *Journal Of Climate,* 26**,** 1654-1668.

Blamey, R. C. & Reason, C. 2012. Mesoscale Convective Complexes Over Southern Africa. *Journal Of Climate,* 25**,** 753-766.

Bopape, M.-J. M., Sebego, E., Ndarana, T., Maseko, B., Netshilema, M., Gijben, M., Landman, S., Phaduli, E., Rambuwani, G. & Van Hemert, L. 2021. Evaluating South African Weather

Service Information On Idai Tropical Cyclone And Kwazulu-Natal Flood Events. *South African Journal Of Science,* 117**,** 1-13.

Briggs, P. 2008. *Greater St. Lucia Wetland Park,* 30° South Publishers.

Chikoore, H., Vermeulen, J. H. & Jury, M. R. 2015. Tropical Cyclones In The Mozambique Channel: January–March 2012. *Natural Hazards,* 77**,** 2081-2095.

Cook, C., Reason, C. J. & Hewitson, B. C. 2004. Wet And Dry Spells Within Particularly Wet And Dry Summers In The South African Summer Rainfall Region. *Climate Research,* 26**,** 17-31.

Crétat, J., Richard, Y., Pohl, B., Rouault, M., Reason, C. & Fauchereau, N. 2012. Recurrent Daily Rainfall Patterns Over South Africa And Associated Dynamics During The Core Of The Austral Summer. *International Journal Of Climatology,* 32**,** 261-273.

De Coning, E., Forbes, G. S. & Poolman, E. 1998. Heavy Precipitation And Flooding On 12-14 February 1996 Over The Summer Rainfall Regions Of South Africa: Synoptic And Isentropic Analyses. *Natl. Wea. Dig,* 22**,** 25-36.

Dinku, T., Funk, C., Peterson, P., Maidment, R., Tadesse, T., Gadain, H. & Ceccato, P. 2018. Validation Of The Chirps Satellite Rainfall Estimates Over Eastern Africa. *Quarterly Journal Of The Royal Meteorological Society,* 144**,** 292-312.

Driver, P., Abiodun, B. & Reason, C. 2019. Modelling The Precipitation Response Over Southern Africa To The 2009–2010 El Niño Using A Stretched Grid Global Atmospheric Model. *Climate Dynamics,* 52**,** 3929-3949.

Driver, P. & Reason, C. 2017. Variability In The Botswana High And Its Relationships With Rainfall And Temperature Characteristics Over Southern Africa. *International Journal Of Climatology,* 37**,** 570-581.

Du, H., Alexander, L. V., Donat, M. G., Lippmann, T., Srivastava, A., Salinger, J., Kruger, A., Choi, G., He, H. S. & Fujibe, F. 2019. Precipitation From Persistent Extremes Is Increasing In Most Regions And Globally. *Geophysical Research Letters,* 46**,** 6041-6049.

Dube, L. & Jury, M. 2000. The Nature Of Climate Variability And Impacts Of Drought Over Kwazulu-Natal, South Africa. *South African Geographical Journal,* 82**,** 44-53.

Dunning, C. M., Black, E. & Allan, R. P. 2018. Later Wet Seasons With More Intense Rainfall Over Africa Under Future Climate Change. *Journal Of Climate,* 31**,** 9719-9738.

Dyson, L. & Van Heerden, J. 2002. A Model For The Identification Of Tropical Weather Systems Over South Africa. *Water Sa,* 28**,** 249-258.

Fairer-Wessels, F. A. 2017. Determining The Impact Of Information On Rural Livelihoods And Sustainable Tourism Development Near Protected Areas In Kwa-Zulu Natal, South Africa. *Journal Of Sustainable Tourism,* 25**,** 10-25.

Fauchereau, N., Pohl, B., Reason, C., Rouault, M. & Richard, Y. 2009. Recurrent Daily Olr Patterns In The Southern Africa/Southwest Indian Ocean Region, Implications For South African Rainfall And Teleconnections. *Climate Dynamics,* 32**,** 575-591.

Favre, A., Hewitson, B., Lennard, C., Cerezo-Mota, R. & Tadross, M. 2013. Cut-Off Lows In The South Africa Region And Their Contribution To Precipitation. *Climate Dynamics,* 41**,** 2331-2351.

Favre, A., Hewitson, B., Tadross, M., Lennard, C. & Cerezo-Mota, R. 2012. Relationships Between Cut-Off Lows And The Semiannual And Southern Oscillations. *Climate Dynamics,* 38**,** 1473-1487.

Funk, C., Peterson, P., Landsfeld, M., Pedreros, D., Verdin, J., Shukla, S., Husak, G., Rowland, J., Harrison, L. & Hoell, A. 2015. The Climate Hazards Infrared Precipitation With Stations—A New Environmental Record For Monitoring Extremes. *Scientific Data,* 2**,** 1-21.

Garstang, M., Kelbe, B. E., Emmitt, G. D. & London, W. B. 1987. Generation Of Convective Storms Over The Escarpment Of Northeastern South Africa. *Monthly Weather Review,* 115**,** 429-443.

Gebrechorkos, S. H., Hülsmann, S. & Bernhofer, C. 2018. Evaluation Of Multiple Climate Data Sources For Managing Environmental Resources In East Africa. *Hydrology And Earth System Sciences,* 22**,** 4547-4564.

Gillett, N. P., Kell, T. D. & Jones, P. 2006. Regional Climate Impacts Of The Southern Annular Mode. *Geophysical Research Letters,* 33.

Globe, T. Team And Others (Hastings, David A., Paula K. Dunbar, Gerald M. Elphingstone, Mark Bootz, Hiroshi Murakami, Hiroshi Maruyama, Hiroshi Masaharu, Peter Holland, John Payne, Nevin A. Bryant, Thomas L. Logan, J.-P. Muller, Gunter Schreier, And John S. Macdonald), Eds., 1999. *The Global Land One-Kilometer Base Elevation (Globe) Digital Elevation Model, Version,* 1**,** 80305-3328.

Harrison, M. 1984. A Generalized Classification Of South African Summer Rain-Bearing Synoptic Systems. *Journal Of Climatology,* 4**,** 547-560.

Hart, N., Reason, C. & Fauchereau, N. 2010. Tropical–Extratropical Interactions Over Southern Africa: Three Cases Of Heavy Summer Season Rainfall. *Monthly Weather Review,* 138**,** 2608-2623.

Hart, N. C., Reason, C. J. & Fauchereau, N. 2012. Building A Tropical–Extratropical Cloud Band Metbot. *Monthly Weather Review,* 140**,** 4005-4016.

Hart, N. C., Reason, C. J. & Fauchereau, N. 2013. Cloud Bands Over Southern Africa: Seasonality, Contribution To Rainfall Variability And Modulation By The Mjo. *Climate Dynamics,* 41**,** 1199-1212.

Hart, R. E. & Grumm, R. H. 2001. Using Normalized Climatological Anomalies To Rank Synoptic-Scale Events Objectively. *Monthly Weather Review,* 129**,** 2426-2442.

Hoell, A., Funk, C., Magadzire, T., Zinke, J. & Husak, G. 2015. El Niño–Southern Oscillation Diversity And Southern Africa Teleconnections During Austral Summer. *Climate Dynamics,* 45**,** 1583-1599.

Hoell, A., Funk, C., Zinke, J. & Harrison, L. 2017. Modulation Of The Southern Africa Precipitation Response To The El Niño Southern Oscillation By The Subtropical Indian Ocean Dipole. *Climate Dynamics,* 48**,** 2529-2540.

Howard, E., Washington, R. & Hodges, K. I. 2019. Tropical Lows In Southern Africa: Tracks, Rainfall Contributions, And The Role Of Enso. *Journal Of Geophysical Research: Atmospheres,* 124**,** 11009-11032.

Jury, M. R., Pathack, B., Wang, B., Powell, M. & Raholijao, N. 1993. A Destructive Tropical Cyclone Season In The Sw Indian Ocean: January-February 1984. *South African Geographical Journal,* 75**,** 53-59.

Kalnay, E., Kanamitsu, M., Kistler, R., Collins, W., Deaven, D., Gandin, L., Iredell, M. & Joseph, D. 1996. The Ncep/Ncar 40-Year Reanalysis Project (1996) Bull. *Am. Meteorol. Soc,* 77**,** 437-471.

Kelbe, B. & Germishuyse, T. 2010. Groundwater/Surface Water Relationships With Specific Reference To Maputaland. *Water Research Commission Report***,** 10.

Klinman, M. & Reason, C. 2008. On The Peculiar Storm Track Of Tc Favio During The 2006–2007 Southwest Indian Ocean Tropical Cyclone Season And Relationships To Enso. *Meteorology And Atmospheric Physics,* 100**,** 233-242.

Knapp, K. R., Ansari, S., Bain, C. L., Bourassa, M. A., Dickinson, M. J., Funk, C., Helms, C. N., Hennon, C. C., Holmes, C. D., Huffman, G. J., Kossin, J. P., Lee, H.-T., Loew, A. & Magnusdottir, G. 2011. Globally Gridded Satellite Observations For Climate Studies. *Bulletin Of The American Meteorological Society,* 92**,** 893-907.

Knapp, K. R., Kruk, M. C., Levinson, D. H., Diamond, H. J. & Neumann, C. J. 2010. The International Best Track Archive For Climate Stewardship (Ibtracs) Unifying Tropical Cyclone Data. *Bulletin Of The American Meteorological Society,* 91**,** 363-376.

Kruger, A. C. & Nxumalo, M. 2017. Historical Rainfall Trends In South Africa: 1921–2015. *Water Sa,* 43**,** 285-297.

Laing, A. G. & Fritsch, J. M. 1993. Mesoscale Convective Complexes In Africa. *Monthly Weather Review,* 121**,** 2254-2263.

Laing, A. G. & Fritsch, J. M. 2000. The Large-Scale Environments Of The Global Populations Of Mesoscale Convective Complexes. *Monthly Weather Review,* 128**,** 2756-2776.

Lindesay, J. 1988. South African Rainfall, The Southern Oscillation And A Southern Hemisphere Semi-Annual Cycle. *Journal Of Climatology,* 8**,** 17-30.

Macron, C., Pohl, B., Richard, Y. & Bessafi, M. 2014. How Do Tropical Temperate Troughs Form And Develop Over Southern Africa? *Journal Of Climate,* 27**,** 1633-1647.

Mahlalela, P., Blamey, R., Hart, N. & Reason, C. 2020. Drought In The Eastern Cape Region Of South Africa And Trends In Rainfall Characteristics. *Climate Dynamics,* 55**,** 2743-2759.

Maidment, R. I., Grimes, D., Allan, R. P., Tarnavsky, E., Stringer, M., Hewison, T., Roebeling, R. & Black, E. 2014. The 30 Year Tamsat African Rainfall Climatology And Time Series (Tarcat) Data Set. *Journal Of Geophysical Research: Atmospheres,* 119**,** 10,619-10,644.

Malherbe, J., Engelbrecht, F. A., Landman, W. A. & Engelbrecht, C. J. 2012. Tropical Systems From The Southwest Indian Ocean Making Landfall Over The Limpopo River Basin, Southern Africa: A Historical Perspective. *International Journal Of Climatology,* 32**,** 1018-1032.

Manhique, A., Reason, C., Rydberg, L. & Fauchereau, N. 2011. Enso And Indian Ocean Sea Surface Temperatures And Their Relationships With Tropical Temperate Troughs Over Mozambique And The Southwest Indian Ocean. *International Journal Of Climatology,* 31**,** 1-13.

Marshall, G. J. 2003. Trends In The Southern Annular Mode From Observations And Reanalyses. *Journal Of Climate,* 16**,** 4134-4143.

Mavume, A. F., Rydberg, L., Rouault, M. & Lutjeharms, J. R. 2009. Climatology And Landfall Of Tropical Cyclones In The South-West Indian Ocean. *Western Indian Ocean Journal Of Marine Science,* 8.

Mulenga, H., Rouault, M. & Reason, C. 2003. Dry Summers Over Northeastern South Africa And Associated Circulation Anomalies. *Climate Research,* 25**,** 29-41.

Munday, C. & Washington, R. 2017. Circulation Controls On Southern African Precipitation In Coupled Models: The Role Of The Angola Low. *Journal Of Geophysical Research: Atmospheres,* 122**,** 861-877.

Muthoni, F. K., Odongo, V. O., Ochieng, J., Mugalavai, E. M., Mourice, S. K., Hoesche-Zeledon, I., Mwila, M. & Bekunda, M. 2019. Long-Term Spatial-Temporal Trends And Variability Of Rainfall Over Eastern And Southern Africa. *Theoretical And Applied Climatology,* 137**,** 1869-1882.

Ndlovu, M., Clulow, A. D., Savage, M. J., Nhamo, L., Magidi, J. & Mabhaudhi, T. 2021. An Assessment Of The Impacts Of Climate Variability And Change In Kwazulu-Natal Province, South Africa. *Atmosphere,* 12**,** 427.

Ndlovu, M. S. & Demlie, M. 2020. Assessment Of Meteorological Drought And Wet Conditions Using Two Drought Indices Across Kwazulu-Natal Province, South Africa. *Atmosphere,* 11**,** 623.

Nel, W. & Sumner, P. 2006. Trends In Rainfall Total And Variability (1970–2000) Along The Kwazulu-Natal Drakensberg Foothills. *South African Geographical Journal,* 88**,** 130-137.

New, M., Hewitson, B., Stephenson, D. B., Tsiga, A., Kruger, A., Manhique, A., Gomez, B., Coelho, C. A., Masisi, D. N. & Kululanga, E. 2006. Evidence Of Trends In Daily Climate Extremes Over Southern And West Africa. *Journal Of Geophysical Research: Atmospheres,* 111.

Nicholson, S. E. 2000. The Nature Of Rainfall Variability Over Africa On Time Scales Of Decades To Millenia. *Global And Planetary Change,* 26**,** 137-158.

Nicholson, S. E. 2018. The Itcz And The Seasonal Cycle Over Equatorial Africa. *Bulletin Of The American Meteorological Society,* 99**,** 337-348.

Nicholson, S. E. & Kim, J. 1997. The Relationship Of The El Niño–Southern Oscillation To African Rainfall. *International Journal Of Climatology: A Journal Of The Royal Meteorological Society*, 17**,** 117-135.

Nicholson, S. E., Some, B., Mccollum, J., Nelkin, E., Klotter, D., Berte, Y., Diallo, B., Gaye, I., Kpabeba, G. & Ndiaye, O. 2003. Validation Of Trmm And Other Rainfall Estimates With A High-Density Gauge Dataset For West Africa. Part Ii: Validation Of Trmm Rainfall Products. *Journal Of Applied Meteorology,* 42**,** 1355-1368.

Nsubuga, F. N. W., Mearns, K. F. & Adeola, A. M. 2019. Lake Sibayi Variations In Response To Climate Variability In Northern Kwazulu-Natal, South Africa. *Theoretical And Applied Climatology*, 137**,** 1233-1245.

Pohl, B. & Fauchereau, N. 2012. The Southern Annular Mode Seen Through Weather Regimes. *Journal Of Climate,* 25**,** 3336-3354.

Pohl, B., Fauchereau, N., Reason, C. & Rouault, M. 2010. Relationships Between The Antarctic Oscillation, The Madden–Julian Oscillation, And Enso, And Consequences For Rainfall Analysis. *Journal Of Climate,* 23**,** 238-254.

Ramjeawon, M., Demlie, M., Toucher, M. L. & Van Rensburg, S. J. 2020. Analysis Of Three Decades Of Land Cover Changes In The Maputaland Coastal Plain, South Africa. *Koedoe,* 62**,** 1-12.

Ramos, A. M., Trigo, R. M. & Liberato, M. L. 2014. A Ranking Of High-Resolution Daily Precipitation Extreme Events For The Iberian Peninsula. *Atmospheric Science Letters,* 15**,** 328-334.

Ramos, A. M., Trigo, R. M. & Liberato, M. L. 2017. Ranking Of Multi-Day Extreme Precipitation Events Over The Iberian Peninsula. *International Journal Of Climatology,* 37**,** 607-620.

Rapolaki, R., Blamey, R., Hermes, J. & Reason, C. 2020. Moisture Sources Associated With Heavy Rainfall Over The Limpopo River Basin, Southern Africa. *Climate Dynamics*, 55**,** 1473-1487.

Rapolaki, R. S., Blamey, R. C., Hermes, J. C. & Reason, C. J. 2019. A Classification Of Synoptic Weather Patterns Linked To Extreme Rainfall Over The Limpopo River Basin In Southern Africa. *Climate Dynamics,* 53**,** 2265-2279.

Reason, C. 2001. Subtropical Indian Ocean Sst Dipole Events And Southern African Rainfall. *Geophysical Research Letters,* 28**,** 2225-2227.

Reason, C. 2016. The Bolivian, Botswana, And Bilybara Highs And Southern Hemisphere Drought/Floods. *Geophysical Research Letters,* 43**,** 1280-1286.

Reason, C. 2017. Climate Of Southern Africa. *Oxford Research Encyclopedia Of Climate Science.*

Reason, C., Allan, R., Lindesay, J. & Ansell, T. 2000. Enso And Climatic Signals Across The Indian Ocean Basin In The Global Context: Part I, Interannual Composite Patterns. *International Journal Of Climatology: A Journal Of The Royal Meteorological Society,* 20**,** 1285-1327.

Reason, C., Hachigonta, S. & Phaladi, R. 2005. Interannual Variability In Rainy Season Characteristics Over The Limpopo Region Of Southern Africa. *International Journal Of Climatology: A Journal Of The Royal Meteorological Society,* 25**,** 1835-1853.

Reason, C. & Jagadheesha, D. 2005. A Model Investigation Of Recent Enso Impacts Over Southern Africa. *Meteorology And Atmospheric Physics,* 89**,** 181-205.

Reason, C. & Keibel, A. 2004. Tropical Cyclone Eline And Its Unusual Penetration And Impacts Over The Southern African Mainland. *Weather And Forecasting,* 19**,** 789-805.

Reason, C., Landman, W. & Tennant, W. 2006. Seasonal To Decadal Prediction Of Southern African Climate And Its Links With Variability Of The Atlantic Ocean. *Bulletin Of The American Meteorological Society,* 87**,** 941-956.

Reason, C. & Mulenga, H. 1999. Relationships Between South African Rainfall And Sst Anomalies In The Southwest Indian Ocean. *International Journal Of Climatology: A Journal Of The Royal Meteorological Society,* 19**,** 1651-1673.

Reason, C. & Rouault, M. 2002. Enso-Like Decadal Variability And South African Rainfall. *Geophysical Research Letters,* 29**,** 16-1-16-4.

Reason, C. & Rouault, M. 2005. Links Between The Antarctic Oscillation And Winter Rainfall Over Western South Africa. *Geophysical Research Letters,* 32.

Reynolds, R. W., Smith, T. M., Liu, C., Chelton, D. B., Casey, K. S. & Schlax, M. G. 2007. Daily High-Resolution-Blended Analyses For Sea Surface Temperature. *Journal Of Climate,* 20**,** 5473-5496.

Richard, Y., Fauchereau, N., Poccard, I., Rouault, M. & Trzaska, S. 2001. 20th Century Droughts In Southern Africa: Spatial And Temporal Variability, Teleconnections With Oceanic And Atmospheric Conditions. *International Journal Of Climatology,* 21**,** 873-885.

Rouault, M., Florenchie, P., Fauchereau, N. & Reason, C. J. 2003. South East Tropical Atlantic Warm Events And Southern African Rainfall. *Geophysical Research Letters,* 30.

Roy, S. S. & Rouault, M. 2013. Spatial Patterns Of Seasonal Scale Trends In Extreme Hourly Precipitation In South Africa. *Applied Geography,* 39**,** 151-157.

Singleton, A. & Reason, C. 2006. Numerical Simulations Of A Severe Rainfall Event Over The Eastern Cape Coast Of South Africa: Sensitivity To Sea Surface Temperature And Topography. *Tellus A: Dynamic Meteorology And Oceanography,* 58**,** 335-367.

Singleton, A. & Reason, C. 2007. Variability In The Characteristics Of Cut-Off Low Pressure Systems Over Subtropical Southern Africa. *International Journal Of Climatology: A Journal Of The Royal Meteorological Society,* 27**,** 295-310.

Steinke, T. & Ward, C. 1989. Some Effects Of The Cyclones Domoina And Imboa On Mangrove Communities In The St Lucia Estuary. *South African Journal Of Botany,* 55**,** 340-348.

Taljaard, J. 1986. Change Of Rainfall Distribution And Circulation Patterns Over Southern Africa In Summer. *Journal Of Climatology,* 6**,** 579-592.

Thoithi, W., Blamey, R. C. & Reason, C. J. 2021. Dry Spells, Wet Days, And Their Trends Across Southern Africa During The Summer Rainy Season. *Geophysical Research Letters,* 48**,** E2020gl091041.

Todd, M. & Washington, R. 1999. Circulation Anomalies Associated With Tropical-Temperate Troughs In Southern Africa And The South West Indian Ocean. *Climate Dynamics,* 15**,** 937-951.

Todd, M. C., Washington, R. & Palmer, P. I. 2004. Water Vapour Transport Associated With Tropical–Temperate Trough Systems Over Southern Africa And The Southwest Indian Ocean. *International Journal Of Climatology: A Journal Of The Royal Meteorological Society,* 24**,** 555-568.

Toté, C., Patricio, D., Boogaard, H., Van Der Wijngaart, R., Tarnavsky, E. & Funk, C. 2015. Evaluation Of Satellite Rainfall Estimates For Drought And Flood Monitoring In Mozambique. *Remote Sensing,* 7**,** 1758-1776.

Usman, M. T. & Reason, C. 2004. Dry Spell Frequencies And Their Variability Over Southern Africa. *Climate Research,* 26**,** 199-211.

Walker, N. 1990. Links Between South African Summer Rainfall And Temperature Variability Of The Agulhas And Benguela Current Systems. *Journal Of Geophysical Research: Oceans,* 95**,** 3297-3319.

Washington, R. & Preston, A. 2006. Extreme Wet Years Over Southern Africa: Role Of Indian Ocean Sea Surface Temperatures. *Journal Of Geophysical Research: Atmospheres,* 111.

Weitz, J. & Demlie, M. 2014. Conceptual Modelling Of Groundwater–Surface Water Interactions In The Lake Sibayi Catchment, Eastern South Africa. *Journal Of African Earth Sciences,* 99**,** 613-624.

Wiston, M. & Mphale, K. M. 2019. Mesoscale Convective Systems: A Case Scenario Of The 'Heavy Rainfall'event Of 15–20 January 2013 Over Southern Africa. *Climate,* 7**,** 73.